National Library
of Canada

Canadian Theses Service

Ottawa, Canada
K1A 0N4

Bibliothèque nationale
du Canada

Services des thèses canadiennes

CANADIAN THESES

THÈSES CANADIENNES

NOTICE

The quality of this microfiche is heavily dependent upon the quality of the original thesis submitted for microfilming. Every effort has been made to ensure the highest quality of reproduction possible.

If pages are missing, contact the university which granted the degree.

Some pages may have indistinct print especially if the original pages were typed with a poor typewriter ribbon or if the university sent us an inferior photocopy.

Previously copyrighted materials (journal articles, published tests, etc.) are not filmed.

Reproduction in full or in part of this film is governed by the Canadian Copyright Act, R.S.C. 1970, c. C-30.

AVIS

La qualité de cette microfiche dépend grandement de la qualité de la thèse soumise au microfilmage. Nous avons tout fait pour assurer une qualité supérieure de reproduction.

S'il manque des pages, veuillez communiquer avec l'université qui a conféré le grade.

La qualité d'impression de certaines pages peut laisser à désirer, surtout si les pages originales ont été dactylographiées à l'aide d'un ruban usé ou si l'université nous a fait parvenir une photocopie de qualité inférieure.

Les documents qui font déjà l'objet d'un droit d'auteur (articles de revue, examens publiés, etc.) ne sont pas microfilmés.

La reproduction, même partielle, de ce microfilm est soumise à la Loi canadienne sur le droit d'auteur, SRC 1970, c. C-30.

THIS DISSERTATION
HAS BEEN MICROFILMED
EXACTLY AS RECEIVED

LA THÈSE A ÉTÉ
MICROFILMÉE TELLE QUE
NOUS L'AVONS REÇUE

NL-339 (r.86/06)

Canada

THE UNIVERSITY OF ALBERTA

THE SYNTHESIS AND DISSOLUTION OF SODALITE:
IMPLICATIONS FOR NUCLEAR WASTE DISPOSAL

BY

KEITH MONTGOMERY

A THESIS

SUBMITTED TO THE FACULTY OF GRADUATE STUDIES AND
RESEARCH IN PARTIAL FULFILMENT FOR THE DEGREE OF
MASTERS OF SCIENCE

DEPARTMENT OF GEOLOGY

EDMONTON, ALBERTA
FALL/1986

Permission has been granted to the National Library of Canada to microfilm this thesis and to lend or sell copies of the film.

The author (copyright owner) has reserved other publication rights, and neither the thesis nor extensive extracts from it may be printed or otherwise reproduced without his/her written permission.

L'autorisation a été accordée à la Bibliothèque nationale du Canada de microfilmer cette thèse et de prêter ou de vendre des exemplaires du film.

L'auteur (titulaire du droit d'auteur) se réserve les autres droits de publication; ni la thèse ni de longs extraits de celle-ci ne doivent être imprimés ou autrement reproduits sans son autorisation écrite.

ISBN 0-315-32384-1

THE UNIVERSITY OF ALBERTA

RELEASE FORM

NAME OF AUTHOR: KEITH MONTGOMERY

TITLE OF THESIS: THE SYNTHESIS AND DISSOLUTION OF SODALITE: IMPLICATIONS FOR NUCLEAR WASTE DISPOSAL

DEGREE: M. SC. GEOLOGY

YEAR THIS DEGREE GRANTED: Fall, 1986

Permission is hereby granted to THE UNIVERSITY OF ALBERTA LIBRARY to reproduce single copies of this thesis and to lend or sell such copies for private, scholarly or scientific research purposes only.

The author reserves other publication rights, and neither the thesis nor extensive extracts from it may be printed or otherwise reproduced without the author's written permission.

Keith Montgomery..........

(Student's signature)

..11508 - 41 Ave..............

(Student's permanent address)

.....EDMONTON.....................

Date: June 9, 1986

THE UNIVERSITY OF ALBERTA

FACULTY OF GRADUATE STUDIES AND RESEARCH

The undersigned certify that they have read, and recommend to the Faculty of Graduate Studies and Research for acceptance, a thesis entitled THE SYNTHESIS AND DISSOLUTION OF SODALITE: IMPLICATIONS FOR NUCLEAR WASTE DISPOSAL submitted by KEITH MONTGOMERY in partial fulfilment of the requirements for the degree of MASTERS OF SCIENCE IN GEOLOGY

Cm. Scarfe
....
(Supervisor)

....
H. Baadsgaard
....
T. H. Etsell
....

....

Date: June 9, 1986

ABSTRACT

The synthesis and aqueous dissolution kinetics of sodalite and iodosodalite have been studied in an attempt to determine if iodosodalite can be readily synthesized and has suitable dissolution behavior under a variety of conditions.

Iodosodalite was synthesized from a stoichiometric mixture of nepheline gel and NaI under a variety of temperature and pressure conditions, ranging from 200°C and 500 bars to 1200°C and 10.5 Kbars. The presence of iodosodalite was verified by X-ray powder diffraction. Small amounts of crystalline nepheline (< 1 wt. %) were also noted in the X-ray diffraction results. The amount of iodine incorporated into idosodalite was calculated by determining the amount of residual NaI remaining in the experimental charges. The yield of the synthesis reaction was found to depend most heavily on the temperature of the experiment and on the duration of the experiment. The maximum iodine incorporation attained at 600°C and ten to fourteen days at 500 bars, simulating hot pressing conditions, was approximately 80% of the theoretical maximum. Higher temperature and pressure experiments suggested that substantial amounts of iodine could be incorporated at these higher temperatures for a given time.

Large scale synthesis of iodosodalite was carried out with a specially constructed hot pressing apparatus. This apparatus allowed up to 15 grams of iodosodalite to be synthesized at one time. The hot pressing synthesis of iodosodalite was carried out in two stages, between which excess NaI was removed.

Approximately 10 to 15 wt. % iodine was therefore incorporated in the hot pressed iodosodalite.

Preliminary dissolution experiments were conducted on a sample of natural sodalite. Dissolution experiments were conducted in distilled water, pH-adjusted and buffered solutions and in artificial brine solutions. The results suggest that the dissolution of natural sodalite is goverened by a combined surface reaction-diffusion mechanism. The release of Na and Cl is goverened initially by the rate at which an Na^+-H^+ exchange reaction occurs at the surface. Over time, H^+ ions migrate by diffusion into the surface and undergo exchange with Na and Cl within the sample. The release of Si and Al to solution is goverened by the rate at which the hydrolyzed residual lattice decomposes. It is proposed that the rate of H^+ onto the surface is controlled by the formation of an electric double layer near the surface. The characteristics of this surface layer are dependent on the solution pH and the substrate. As a result, there is a minimum rate of dissolution at a solution pH of approximately 8.

The dissolution of iodosodalite was found to be significantly different than the dissolution of natural sodalite. Measurement of the rate of dissolution was complicated by the fact that a soluble Na-silicate was being prefferntially leached. However, it was found that iodine was not being preferentially leached from iodosodalite as chlorine was from natural sodalite. Surface analysis by SIMS did not show the existence of an Na-I leached

layer analogous to the Na-Cl leached layer found in natural sodalite samples.

It is concluded that iodosodalite is a promising candidate wasteform for the geological disposal of radioactive I-129. Iodosodalite can be readily synthesized at temperatures and pressures feasible in an industrial process. Although the rate of iodine release from iodosodalite was difficult to determine, it was found to be comparable to the steady-state release of chlorine from natural sodalite. The fact that iodine is not preferentially leached from iodosodalite implies that the release rate obtained could be used in long term simulation studies of iodosodalite dissolution in a proposed geological repository. Such studies should be conducted in the near future.

ACKNOWLEDGEMENTS

The research for this thesis was carried out under a contract from Atomic Energy of Canada, as part of the Canadian Nuclear Waste Management Program. The research was conducted at the Department of Geology, University of Alberta.

I would like to thank Prof. C.M. Scarfe for supporting me as a graduate student for the duration of the project and for providing much advice and encouragement. Dr. J.T. Dunn assisted with much of the analytical work and provided input for the interpretations.

I would also like to acknowledge Dr. P.J. Hayward of Whiteshell Nuclear Research Establishment for providing technical assistance and for carrying out the SIMS analyses.

TABLE OF CONTENTS

CHAPTER PAGE

1. INTRODUCTION 1
 The Canadian nuclear waste management program 1
 Previous work on candidate wasteforms 3
 Objectives 6
2. SYNTHESIS OF IODOSODALITE 7
 Structure and composition of sodalite 7
 Synthesis of sodalite 10
 Characterization of iodosodalite 15
 Large scale synthesis of iodosodalite 24
 Conclusions 29
3. DISSOLUTION OF NATURAL SODALITE 31
 Introduction 31
 Brief review of chemical kinetics 32
 Previous silicate dissolution studies 35
 Sample preparation 40
 Experimental method 41
 Results 44
  Distilled water experiments 44
  Initial pH experiments 60
  Buffered pH experiments 60
  Synthetic brine experiments 69

CHAPTER PAGE

SIMS analysis of wafer surfaces 69
Discussion 81
Conclusion 96
4. DISSOLUTION OF IODOSODALITE 100
Introduction 100
Sample preparation 101
Experimental method 101
Description of experiments 103
Results 103
Distilled water experiments 105
Synthetic brine experiments 114
Discussion 115
Conclusions 118
5. CONCLUSIONS 120
BIBLIOGRAPHY 123
APPENDIX 1. THE GEL METHOD 130
APPENDIX 2. METHODS OF SOLUTION ANALYSIS 133

LIST OF TABLES

Table	Description	Page
1	Iodosodalite synthesis experiments	14
2	Iodosodalite unit cell parameters	16
3	Composition of natural sodalite sample used in the dissolution experiments	39
4	Chemical compositions of synthetic brines	42
5	Solution analyses of distilled water experiments	46
6	Regression analysis of the distilled water experimental data	58
7	Solution analyses of initial pH experiments	61
8	Solution analyses of the buffered pH experiments	64
9	Rate laws for the release of Na, Al, Si and Cl in pH buffered solutions	68
10	Iodosodalite dissolution experiments in distilled water	104
11	Rate laws parameters for iodosodalite dissolution in distilled water	108
A1	Electron microprobe analysis of nepheline gel	132

LIST OF FIGURES

Figure		Page
1.	The crystalline structure of sodalite (after Pauling, 1930).	8
2.	X-ray powder diffraction pattern of iodosodalite	19
3.	Iodosodalite reaction yield with increasing temperature	22
4.	Schematic of hot pressing apparatus	25
5.	Solution analyses for first set of distilled water dissolution experiments	48
6.	Solution analyses for second set of distilled water dissolution experiments	50
7.	Solution analyses for initial pH experiments	62
8.	Solution analyses for buffered pH experiments	66
9.	SIMS profiles of leached natural sodalite	76
10.	Comparison of actual and model SIMS profiles	92
11.	Solution analyses for dissolution of iodosodalite in distilled water	106
12.	SIMS profile of leached iodosodalite	112

LIST OF PHOTOGRAPHIC PLATES

Plate	Description	Page
1	Iodosodalite crystals from synthesis experiments	17
2	Surfaces of natural sodalite wafers leached for varying times in distilled water	52
3	Surfaces of natural sodalite wafers leached in artificial brines	70
4	Surface of an iodosodalite disk leached in distilled water	110

CHAPTER 1. INTRODUCTION

This thesis deals with the synthesis and dissolution of sodalite and the implications for the disposal of ^{129}I nuclear waste. The study was supported by Atomic Energy of Canada Ltd., and set out to obtain data on the suitability of sodalite as a wasteform for radioactive ^{129}I. The study involved the synthesis of sodalite under high temperature and pressure conditions and a study of its dissolution kinetics in distilled water and saline brines. In the following paragraphs I briefly review the scientific and technological considerations involved in selecting a wasteform for the disposal of ^{129}I, and define the scientific objectives of this thesis.

The Canadian Nuclear Waste Management Program

The radioisotope ^{129}I is formed by the β^- decay of ^{129}Te in the fuel cycle of nuclear reactors. ^{129}I has a half-life of 1.7×10^7 y and decays to radioactive ^{129}Xe by the emission of a 0.189 MeV β^- particle. Approximately 0.04g of ^{129}I is produced per Kg of CANDU nuclear fuel (Lemire, 1978). Although ^{129}I is only weakly radioactive, its long half-life end affinity for the thyroid gland indicates that special consideration must be given to its disposal.

The Canadian nuclear waste management program is currently investigating the problems of disposing nuclear wastes in large underground repositories. The repository would likely be situated in a granitic pluton somewhere in the Canadian Shield (Boulton, 1978). The nuclear waste would be surrounded by several barriers designed to minimize the contact of groundwater with the waste (Bird, 1982). It is thought that the integrity of such a repository would last for periods of time in excess of 1000 years. This would allow most of the very radioactive wastes to decay down to acceptable concentrations.

In this strategy it is assumed that groundwater will eventually penetrate the repository and barriers and begin attacking the wasteforms. A complete assessment of the suitability of a candidate wasteform must therefore include a study of its stability in groundwaters likely to enter the repository. The timescale on which this is likely to occur is small compared to the half-life of ^{129}I. Hence, most of the iodine waste will be present in the wasteform when the repository is breached, and will eventually migrate into the biosphere (McKay _et. al._, 1981). This has led several researchers to formulate different criteria for the disposal of ^{129}I. Burger (1980) has studied the distribution and movement of natural iodine in the biosphere. He concludes that the most effective method for disposing of ^{129}I is by finding a wasteform which will release the iodine at a sufficiently low rate while assuring that the ^{129}I is isotopically diluted by stable ^{127}I to safe levels. Thus the problem of disposing of ^{129}I becomes one of finding a wasteform which will release iodine slowly under chemical attack and assuring that the ^{129}I will be sufficiently diluted by stable iodine before it enters food or water consumed by humans. Determining whether a wasteform is suitable for fixing ^{129}I will require detailed modelling of the release rate in combination with modelling which is specific to the repository. Such modelling will not be attempted here.

Previous work on candidate wasteforms

McKay _et. al._ (1981) have reviewed the different compounds which have been proposed as potential wasteforms for ^{129}I. In assessing the proposed wasteforms they set down seven criteria which were used in the review process. These criteria are summarized below:

1. Resistance to alteration in the repository environment. The wasteform should be stable under the pressure and temperature conditions in the repository. The rate of iodine release should be minimal in groundwaters likely to enter the repository.
2. Development of a suitable method for preparing the wasteform. The wasteform should be easily synthesized with materials which are readily available and under industrially feasible conditions. The wasteform should incorporate a large amount of iodine, preferably bonded into the wasteform chemical structure. The amount of materials recycling should also be minimized.

Since ^{129}I is not very radioactive and the decay energy is low, radiolytic damage to the wasteform will be minimal. However, radiolytic damage to the wasteform from other wastes should be avoided by locating the ^{129}I waste some distance from other wastes, and perhaps in a separate repository.

The wasteforms suggested for ^{129}I can be grouped into four categories (McKay _et. al._, 1981):

1. Inorganic iodides and iodates.
2. Solid sorbents, e.g. zeolites loaded with iodine.
3. Cement incorporating forms of (1) and (2).
4. Low melting point glasses.

There are many iodides and iodates which are sufficiently insoluble to act as candidate wasteforms. Examples include AgI, Hg_2I_2, $Ba(IO_3)_2$ (Burger _et. al._, 1981). However, many of these compounds become quite soluble with increasing temperature, and could become unstable in the repository. Several compounds also undergo reduction/oxidation reactions which result in the release of iodine to solution. These compounds should also be discarded. In the final assessment, McKay _et. al._ (1981) conclude that AgI and $Ba(IO_3)_2$ are the iodine compounds best suited for ^{129}I disposal.

Very little research has been done on the stability of iodine-bearing zeolites in groundwaters. It is thus hard to assess the suitability of these compounds. However, many zeolites can incorporate sizable amounts of iodine (Barrer, 1982), although they have the tendency to ion exchange readily with aqueous solutions (Barrer, 1982).

The incorporation of iodides and iodates into cement has been suggested as a possible way of consolidating waste (Clark, 1977). However, many iodides and iodates are unstable at the pH conditions produced during the production of the cement, releasing iodine. In addition, cements have not proved very resistant to chemical alteration (McKay _et. al._, 1981), although researchers are investigating the effects of addition of chemicals to inhibit the release of iodine. Further assessment awaits the results of these experiments.

Iodine could also be incorporated in low melting point glasses. However, the glasses melt at a temperature which is sure to cause considerable iodine volatilization or the breakdown of the iodine compounds. The end effect is that considerable reprocessing may be required to recycle the volatilized iodine. In addition, studies on the dissolution of glasses have shown that they possess limited resistance to chemical attack. Other glasses may be developed which overcome both the volatilization problem and the chemical resistance problem (McKay _et. al._, 1981).

There are other silicate minerals besides zeolites which can incorporate large amounts of volatiles, including iodine, in their crystal structures. The mineral sodalite

($Na_8Al_6Si_6O_{24}Cl_2$) incorporates 7.32 wt % Cl into its lattice. Barrer and White (1952) and Tomisaka and Eugster (1968) have synthesized iodine-bearing sodalite. Strachan and Babad (1979) also synthesized iodine sodalite and conducted preliminary leaching tests which indicated that it could also be a candidate wasteform for the disposal of ^{129}I.

Objectives

This study will investigate the synthesis and dissolution of iodine sodalite. In particular, the criteria outlined by McKay et. al. (1981) will be used as a guide in the study. The overall goals will be to:

1. determine under what conditions iodine sodalite can be synthesized and how much iodine can be routinely incorporated.
2. determine the release rate of iodine in a variety of solutions.
3. understand the dissolution kinetics of sodalite and iodosodalite.

This strategy outlines the three different studies undertaken for this project. Each of the goals will be described further in the following chapters.

CHAPTER 2. SYNTHESIS OF IODOSODALITE

Structure and composition of sodalite

The structure of sodalite was described in detail by Pauling (1930) and Barth (1932). The structure was found to be cubic and belongs to the space group P43n. Pauling (1930) determined the structural formula to be $Na_8Al_6Si_6O_{24}Cl_2$ (Fig. 1). The Si and Al atoms are in tetrahedral coordination, and are bonded together to form a large truncated octahedral cage (Deer *et. al.*, 1963). Each Si atom has four Al next nearest neighbors at an average distance of 3.14A (Pauling, 1930). Similarly, each Al atom has four Si next nearest neighbors at the same distance. The aluminosilicate framework comprises six four-membered rings and eight six-membered rings (Deer *et. al.*, 1963). The cage structures are stacked in the form of a cube in such a way that each six-membered ring is shared between two cages. Sodium cations lie along the diagonals of the unit cell, and are coordinated by four anions; one Cl at 2.70A and three framework O atoms at 2.36A. Each cage structure contains one Cl anion, which is tetrahedrally coordinated by the four nearest Na cations (Pauling, 1930).

The unit cell is defined by the positions of eight Cl anions, which are located at the apices of a cube. Pauling (1930) calculated that the unit cell should have an edge length

Figure 1. The crystal structure of sodalite ($Na_8Si_4Al_4O_{24}Cl_2$). The primary cage structure is shown here. The shaded circles indicate Cl^- ions while the unshaded circles are Na^+ ions. The tetrahedra are either SiO_4 or AlO_4 anions. Diagram adapted from Pauling (1930).

Sodalite ($Na_8 Al_6 Si_6 O_{24} Cl_2$)

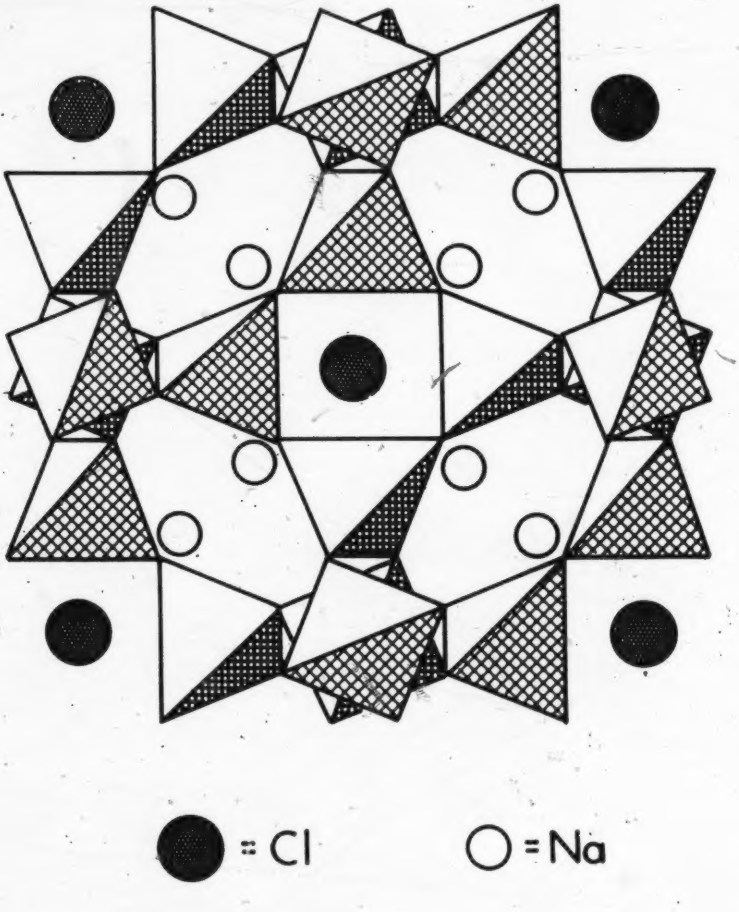

of about 9.4A, but observed a length of 8.87A. Pauling explained this difference by noting that the Na and Cl ions do not completely fill their respective sites, and thus allow the aluminosilicate structure to collapse partially. Pauling suggested that replacement of Na and Cl ions by ones of different sizes should cause a variation in the unit cell edge length. This was, in fact, observed by Jaeger and van Melle (1927), who replaced the Na by larger alkali cations (K, Rb, Cs) and found that the edge length increased to 9.4A. Tomisaka and Eugster (1968) replaced the Cl anion with OH, Br and I, and found that the edge length increased from 8.93 for hydroxysodalite to 9.01A for iodine-bearing sodalite. Thus the dependence of unit cell edge length on the sizes of interframework ions has been demonstrated.

Chemical analyses of natural sodalites (Deer et. al., 1963; Taylor, 1967) indicate that the ideal formula $Na_8Al_6Si_6O_{24}Cl_2$ is closely approached. Replacement of Na by K and Ca is quite restricted, and in most cases is less than 10 cation percent. Chloride is by far the most abundant anionic species, being at least an order of magnitude greater in concentration than other species such as SO_4^{-2} and OH^-. The replacement of Al^{+3} by Fe^{+3} and of Si^{+4} by Ti^{+4} is also very limited.

Synthesis of Sodalite

Sodalite is easily synthesized from a wide variety of starting materials and under a considerable range of pressure and temperature conditions. Stormer and Carmichael (1971), in determining the free energy of formation of sodalite found that its field of stability depends on the activities of SiO_2 and Cl. They reported that sodalite is only stable in silicic magmas where the SiO_2 activity is below the nepheline-albite equilibrium. Stormer and Carmichael (1971) also found that under conditions where the fugacity of fluorine is sufficiently high with respect to the fugacity of Cl, halide phases such as villiaumite (NaF) or fluorite will form with nepheline instead of sodalite. Prener and Ward (1950) produced sodalite by heating stoichiometric mixtures of Na_2CO_3, Al_2O_3, SiO_2 and NaCl at 900°C in a nitrogen atmosphere. Barrer and White (1952) synthesized sodalite by crystallization from a gel produced by mixing a suspension of kaolinite and NaCl solution and heating until dry. Barrer _et. al._ (1968) synthesized sodalite by reacting kaolinite with hydroxide solutions of Li, Na, K, Rb and Cs at 110°C. Van Peteghem and Burley (1960) synthesized sodalite by mixing nepheline and NaCl in the molar ratio 3Ne:1NaCl and reacting the mixture in the presence of water at a temperature of 600°C. Tomisaka and Eugster (1968) also used nepheline, but used NaBr, NaI and NaOH in addition to NaCl. Other synthetic sodalite compositions have been reported by Barrer and Falconer (1956), including basic sodalite, lithium basic sodalite and silver basic sodalite, where OH^- replaces

Cl^-. Schipper and Lathouwers (1972) synthesized sodalite containing approximately 14 wt.% Br in place of Cl. Finally, Strachan and Babad (1979) synthesized iodine-bearing sodalite using the method of Barrer and White (1952) to study its suitability as a host for ^{129}I.

Iodine sodalite was synthesized following the method of Tomisaka and Eugster (1968). Nepheline was prepared as a gel (Hamilton and Henderson, 1967; Biggar and O'Hara, 1969). Details of the gel preparation can be found in Appendix 1. Nepheline gel and NaI were mixed in the molar proportions 3Ne:1NaI and reacted under a variety of pressure and temperature conditions to synthesize iodine-bearing sodalite (hereafter called iodosodalite). All experimental charges were contained in sealed noble metal or graphite capsules. A high temperature muffle furnace was used for one atmosphere experiments, cold-seal pressure vessels (Tuttle and Bowen, 1949) were used for intermediate pressure experiments, and high pressure experiments were conducted in a piston-cylinder device (Boyd and England, 1960).

Welded Pt capsules were used in the one atmosphere muffle furnace experiments to prevent volatilization of iodine. The temperature inside the furnace was known to ±20°C. A chromel-alumel thermocouple was used to monitor and control the furnace temperature and to control the furnace setting.

Welded Ag capsules were used in the cold-seal pressure vessel experiments. Silver was chosen as a capsule material because it is less permeable to hydrogen than other noble metals (Edgar, 1973), decreasing the possibility of hydration of the sample. Kanthal-wound resistance furnaces which completely surrounded the the pressure vessel were used. The furnace was controlled by a thermocouple which was in close proximity to the pressure vessel. The temperature inside the pressure vessel was measured with a chromel-alumel thermocouple inserted into a cavity in the vessel, and is accurate to ±5°C. Pressures were measured with Bourdon-tube gauges which had been previously calibrated against a Heise gauge, believed accurate to ±0.1 Kbars.

High pressure experiments were performed with a piston-cylinder device (Boyd and England, 1960). Experiments were conducted in sealed Pt or graphite capsules. The graphite capsules were used in later experiments because they allowed larger samples (100-200 mg) to be loaded and run. Temperatures, measured with a Pt-PtRh$_{13}$ thermocouple which was within 0.5mm of the capsule, are accurate to ±10°C. Tapered graphite furnaces were used to minimize thermal gradients inside the capsule.

The experimental durations listed in Table 1 represent the time for which the experiment was at the run conditions. At the end of a run the temperature was decreased to room temperature (25°C) as quickly as possible to limit the amount of reaction

Table 1. Iodosodalite Synthesis Experiments

Number	duration, d	T, °C	P, kbar	Yield, %
Iso3	0.04	1200	10.5	73
Iso4	0.08	1200	10.5	82
Iso5	6.92	600	0.5	86.6
Iso6	13.98	600	0.5	71.8
Iso8	7.01	200	0.5	37
Iso9	7.02	500	0.5	70.4
Iso10	0.99	600	0.5	76.5
Iso11	2.0	600	0.5	75.1
Iso12	2.88	600	0.5	81
Iso14	10.13	600	0.5	87.8
Iso16	0.99	200	0.5	57
Iso21	1.0	300	0.5	38.5
Iso22	2.04	400	0.5	58.7
Iso24	2.04	400	0.5	59.1
Iso25	2.04	300	0.5	50
Iso28	1.0	500	0.5	74.8
Iso34	1.0	400	0.5	62.8
Iso35	1.0	300	0.5	59.9

occurring after the end of the experiment. The one atmosphere experiments were quenched in a stream of cool air, and were brought down to 25°C within one minute. Cold seal pressure vessel experiments were also quenched with air down to 40°C, but over a five minute period. The actual cooling rate is highly non-linear, varying from about 50°C/sec at 600°C to 2-3°C/sec at 100°C. However, the time required to reach 100°C was only about 3 minutes. Piston cylinder experiments were quenched by switching off the electrical current supplied to the graphite furnace. This resulted in cooling rates of about 100°C/sec. Isobaric quenches were not employed in the elevated pressure experiments because the volatile content of the charges was minimal.

Characterization of Iodosodalite

The results of the synthesis experiments are presented in Table 1. The presence of iodosodalite was confirmed by X-ray powder diffraction, using the pattern reported by Tomisaka and Eugster (1968) (see Fig. 2). The X-ray diffraction data were reduced using the program of Appleman et. al. (1963). Calculated unit cell edge lengths and volumes compared quite favorably with those presented in Tomisaka and Eugster (1968), there being only a 5% difference in the values (Table 2). The unit cell volume is 728.99 ± 0.36 A^3, and there is one formula unit per unit cell. The calculated density of iodosodalite is therefore

Table 2. Iodosodalite unit cell parameters

	This study	Tomisaka and Eugster, 1968
Edge length	8.99±0.02 A	9.014±0.002 A
Cell volume	728.99±0.36 A^3	732.41 A^3

Plate 1. Scanning electron microscope photomicrograph of iodosodalite crystals produced in a synthesis experiment (600°C, 500 bars, 10 days). The larger crystals are approximately 2 um across. The characteristic isometric crystal form of iodosodalite is clearly visible.

Figure 2. The X-ray powder diffraction pattern of iodosodalite. The horizontal axis is graduated, showing increasing 2θ angle to the left. The individual peaks are labelled with the phase responsible and the corresponding atomic spacing. Iodosodalite peaks are designated by ISO and nepheline peaks by Ne. National Bureau of Standards No. 640 silicon powder was used as a calibration standard. Analytical conditions: Cu K_α radiation, 0.5° 2θ per minute, 1° slits.

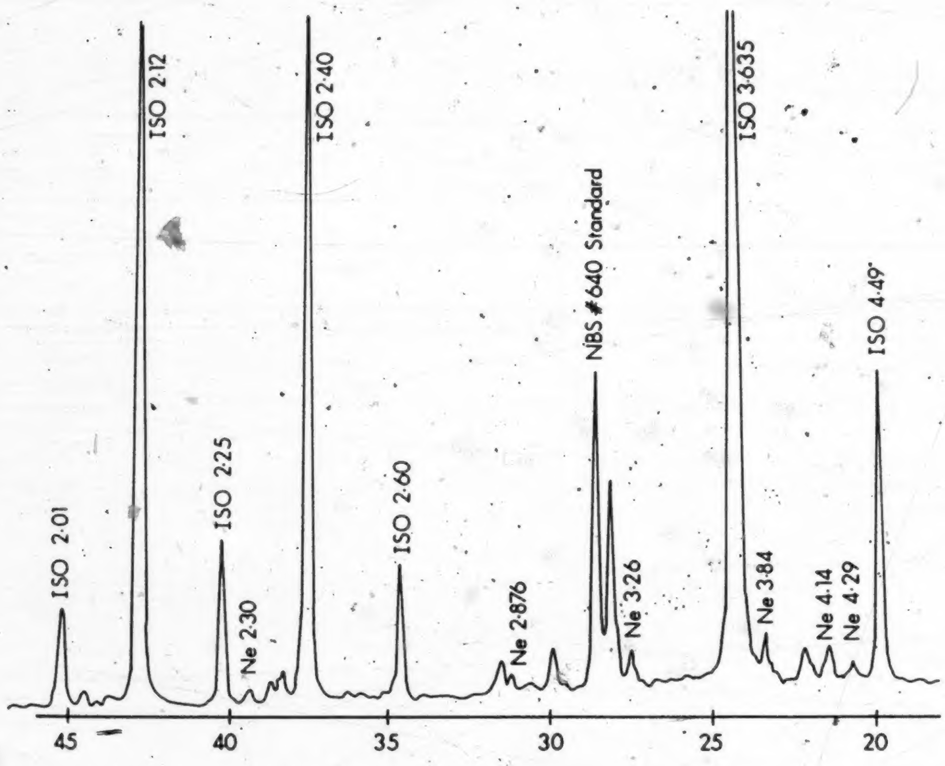
ISO 2·01
ISO 2·12
ISO 2·25
Ne 2·30
ISO 2·40
ISO 2·60
Ne 2·876
NBS #640 Standard
Ne 3·26
ISO 3·635
Ne 3·84
Ne 4·14
Ne 4·29
ISO 4·49
45
40
35
30
25
20

2.63 ± 0.02 g cm^{-3}.

Scanning electron microscope photomicrographs showed well formed isometric crystals with an average width of about two microns (Plate 1).

In several of the short duration cold seal pressure vessel experiments, the X-ray diffraction pattern indicated that some nepheline had crystallized (Fig. 2). This indicated that not all of the NaI in the charge had been incorporated into iodosodalite.

To determine how much NaI had been incorporated into iodosodalite in each of the experiments, a technique was developed to measure the amount of unreacted NaI. A known amount of finely crushed experimental charge was weighed onto a Whatman GF/F filter paper, which traps all particles larger than two microns in diameter. The powder was then rinsed thoroughly with distilled water and acetone, and dried in an oven at 110°C. The weight change was then noted. It was assumed that the change in weight was entirely due to dissolution of NaI during rinsing. The weight fraction of NaI in the original unreacted mixture is known, and the ratio of the weight change to the weight of NaI originally present is a measure of the extent of reaction. The results are presented in Table 1 and Figure 3. A 20% difference in calculated yield was obtained for samples from the same experimental charge and this is taken to be the error involved in the method. Some of the weight loss may have been caused by removal of very fine iodosodalite particles during rinsing.

Figure 3. Iodosodalite reaction yield with increasing temperature. The yield of the reaction is defined as the percentage of the amount of NaI initially present that is incorporated into iodosodalite. The yield calculation is described in the text. Several different duration experiments are shown on the figure. The experimental durations in days are shown next to each symbol type.

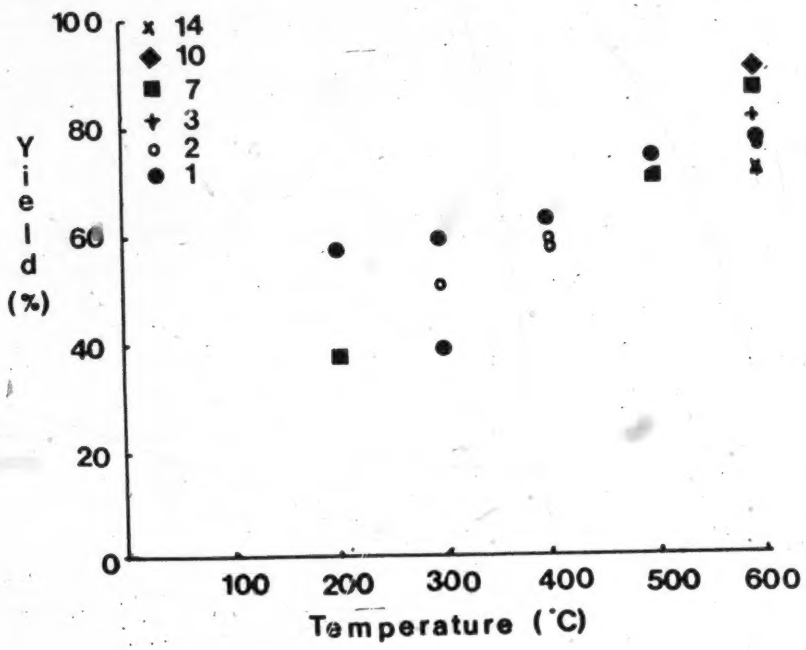

x 14
◆ 10
■ 7
+ 3
o 2
● 1
Yield (%)
100
80
60
40
20
0
100
200
300
400
500
600
Temperature (°C)

On the basis of the synthesis experiments, it is concluded that the optimum conditions for the synthesis of iodosodalite are 600°C and a duration of two days. Pressure does not appear to be a significant factor in the synthesis in view of the range over which iodosodalite can be produced. Large-scale production of iodosodalite can therefore be conducted at these conditions.

Large scale synthesis of iodosodalite

Large amounts of iodosodalite must be produced for dissolution studies. The method chosen for this in the present study is hot pressing. This technique allows large amounts of material to be synthesized inexpensively.

Hot pressing has been previously studied as a means of synthesizing iodosodalite by Winters (undated) and Strachan and Babad (1979). Winters found that iodosodalite synthesized under temperatures in excess of 1000°C and pressures of 5000-7000 p.s.i. (340-480 Kbar.) had a density of 2.6 g cm^{-3} and incorporated 15-20 wt% iodine. Strachan and Babad (1979) did not find any iodine volatilization during hot pressing.

A diagram of the hot pressing apparatus constructed for this study is shown in Figure 4. The sample capsule is constructed from 1.6 cm diameter silver tubing in the following way: (1) a length of the tubing (approximately 5 cm) is annealed at 800°C for 30 minutes; (2) a flat piece of silver is welded onto one end of the tubing; (3) the capsule is machined to fit into the cylinder; and (4) the capsule is boiled in dilute HCl to remove

Figure 4. Schematic diagram of the hot press apparatus constructed for the large scale synthesis of iodosodalite. The retaining cylinder, pistons and end-caps are composed of Rene-41 alloy. The furnace surrounds the retaining cylinder. Pressure is supplied by an Enerpac RWT-40 hydraulic cylinder and pump. The furnace is controlled by a simple on-off controller. Only the retaining cylinder, pistons and end-caps are drawn to scale.

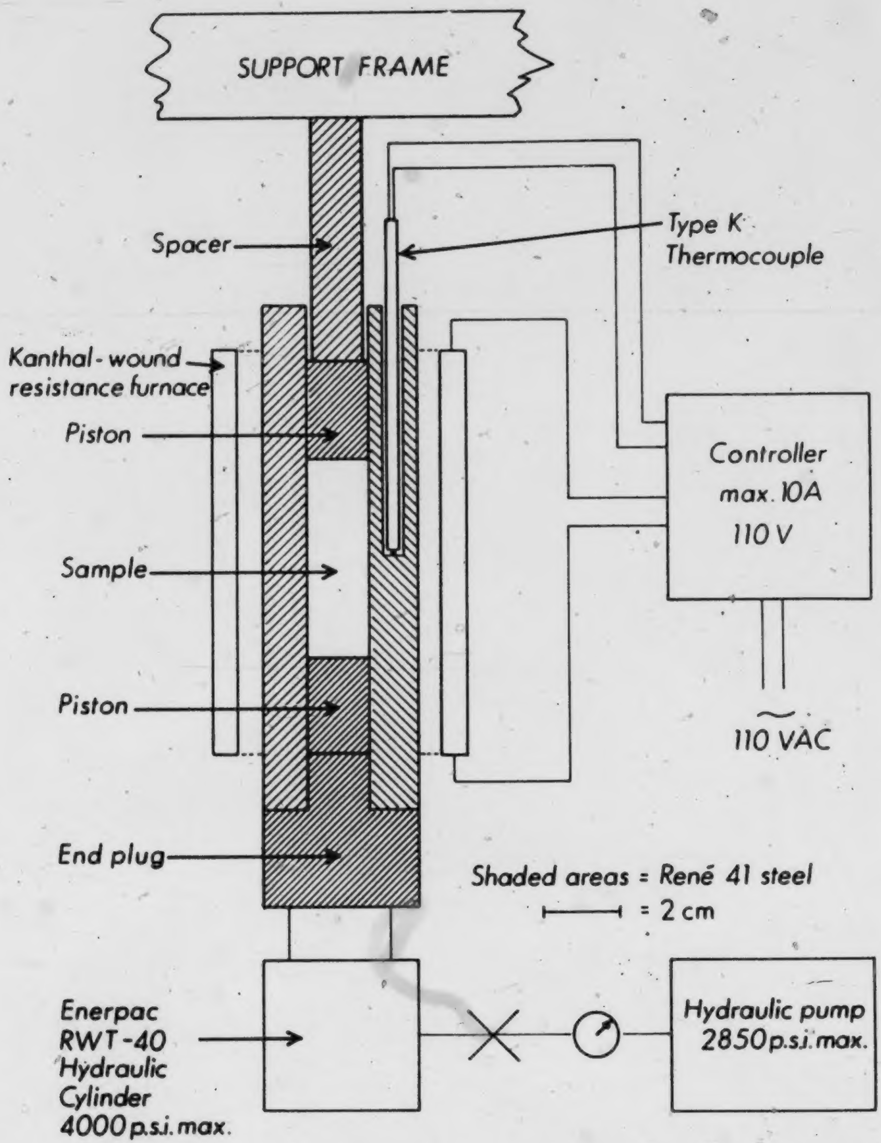
SUPPORT FRAME
Spacer
Type K Thermocouple
Kanthal-wound resistance furnace
Piston
Controller
max. 10A
110 V
Sample
Piston
110 VAC
End plug
Shaded areas = René 41 steel
= 2 cm
Enerpac RWT-40 Hydraulic Cylinder 4000 p.s.i. max.
Hydraulic pump 2850 p.s.i. max.

any contaminants.

An Enerpac RWT-40 hydraulic cylinder connected to an Enerpac P-18 hydraulic hand pump supplies pressures of up to 500 bars to the sample. Pressure was measured by a small gauge attached to the hydraulic line between the cylinder and pump. The pressure imposed on the sample was not calibrated against gauge pressure, but was approximated by ratioing the square of the piston radius againat the square of the hydraulic cylinder piston radius. The actual sample pressure depends on how well the silver capsule transmits the pressure. Under pressure the silver capsule will be compressed, and in this way transfers pressure to the sample. If there is significant friction between the silver capsule and the side of the sample volume, the actual pressure transferred to the sample could be considerably less than the approximation from the ratio of radii.

The pressure vessel is heated by a cylindrical Kanthal wound resistance furnace which is controlled by a 110V-10A on/off controller. Temperature is monitored by a type K (chromel-alumel) thermocouple situated in a cavity in the pressure vessel cylinder. The furnace and controller can heat to temperatures of 1000°C, but beyond this the Rene 41 alloy begins to weaken.

Approximately 10 g of nepheline-NaI mixture, prepared by the method discussed in the previous section, is loaded into the capsule which is then capped with a disk of silver. Before hot pressing, the sample was cold pressed in the capsule with a 12 ton hydraulic jack. This cold pressing stage served to seal the unwelded end of the capsule and remove any remaining void space.

After cold pressing, the pressure vessel was inserted into the hot press frame and brought up to hot pressing run conditions (700°C, approx. 450 bars). The time required to reach temperature was about two hours. The pressure required frequent trimming as the valves did not seal completely. Consequently, the pressure range for the synthesis runs is 250-450 bars.

The synthesis run was ended after 48 hours by turning the controller off and allowing the furnace to cool to room temperature, requiring approximately three hours. The hot pressed material was removed from the capsule and crushed and rinsed with distilled water. Reaction yields at this time were 50 to 70%. To complete the synthesis the rinsed powder was hot pressed again under the same conditions for 48 hours.

The final product is a fine-grained polycrystalline aggregate with a density of 2.27 ± 0.06 g cm^{-3} and a Vickers Hardness of $VHN_{100g}=400$, equivalent to a Mohs hardness of approximately 5. The difference between the calculated and measured density is attributed to residual void space between the grains. X-ray powder diffraction of the final product showed only iodosodalite with minor nepheline (Fig. 3). No trace of NaI was observed. The presence of nepheline would not alter the density since the density of nepheline (2.56-2.66, Deer _et. al._,

1965) is similar to that of iodosodalite.

Conclusions

A series of iodosodalite synthesis experiments were conducted over the temperature range 200-1200°C and over the pressure range 1 atm to 10.5 Kbars. The durations of the experiments were between 1 hour and 14 days. The presence of iodosodalite was verified by X-ray diffraction. In addition to iodosodalite, small amounts of residual NaI and nepheline were found to occur in the experimental charges.

The iodosodalite synthesis reaction was found to be less than 100% efficient over the pressure-temperature-time interval studied. The amount of iodine incorporated in iodosodalite was found to be largely dependent on the temperature, and experimental duration was found to be of secondary importance. Maximum incorporation of iodine (80% of theoretical maximum) was achieved after 10 to 14 days, although relatively large amounts (50-70%) were incorporated after three days at 600°C. Therfore, it was concluded that large amounts of iodine could be incorporated in iodosodalite after three days if the temperature was above 600°C.

The hot pressing synthesis of iodosodalite was carried out in two stages. During the first stage, the mixture of nepheline and NaI was reacted at 600°C and 300-400 bars for 72 hours. This resulted in an iodosodalite yield of approximately 70%. The product was then crushed and rinsed with distilled water to remove any remaining NaI, and thoroughly dried at 110°C. The second stage involved hot pressing the rinsed mixture at 700°C and 300 bars for 48 hours to complete the reaction and consolidate the mixture.

The final product was examined by X-ray diffraction, and was found to be composed of iodosodalite with small amounts of nepheline. No residual NaI was detected. Based on the reaction yields of these two steps, the final product contains between 11 and 15 wt% iodine and a density of 2.27 g cm^{-3}. The density of iodosodalite synthesized for this study is somewhat lower than the theoretical maximum (2.6 g cm^{-3}) and is attributed to residual void space between the grains.

Based on this study it is concluded that hot pressing is a satisfactory technique for the large scale synthesis of iodosodalite. The temperatures and pressures required for this method can be attained with commercially available equipment.

CHAPTER 3. THE DISSOLUTION OF NATURAL SODALITE

Introduction

The dissolution behavior of several silicate mineral groups has been previously investigated and several theories have been developed to explain these observations. The feldspar minerals have been the most extensively studied (e.g. Wollast, 1967; Helgeson, 1971; Busenberg and Clemency, 1976; Holdren and Berner, 1978; Aagaard and Helgeson, 1982; Helgeson et al. 1985), although other mineral groups, such as quartz (e.g. Rimstidt and Barnes, 1980) and the magnesium silicates (e.g. Luce et al. 1972; Grandstaff, 1979) have also been examined. To date, three major theories of silicate dissolution have been proposed. Two of the theories assume that diffusion through a surface layer is the rate controlling process (Wollast, 1967; Busenberg and Clemency, 1976; Chou and Wollast, 1985), while the third assumes that a surface reaction is the rate limiting step (Lagache, 1976; Holdern and Berner, 1978; Aagaard and Helgeson, 1982; Helgeson et al., 1985). Each of these theories has some theoretical basis, and each can explain some particular aspect of the dissolution process. These theories will be examined in depth below.

The study of the dissolution kinetics of silicate minerals is of immense importance to the study of low temperature geochemistry and diagenesis (Berner, 1978 and 1981; Lasaga, 1981). It also has application to the disposal of nuclear wastes, where an attempt is made to find the wasteform that is most resistant to chemical attack (Fung and Sanipelli, 1982; Fleer, 1983). Since sodalite has been proposed as a candidate for the disposal of ^{129}I nuclear waste (Strachan and Babad, 1979), it is necessary to examine the dissolution of natural sodalite in order to determine what factors will be of importance. In particular, it is necessary to determine if sodalite is a stable phase under conditions likely to be present in the storage vault.

Brief Review of Chemical Kinetics

In the following sections reference will be made to fundamental principles of chemical kinetics. In particular arguments and descriptions from transition state theory (Glasstone *et al.*, 1941) will be used. The essential definitions and equations will be presented below.

The rate of a chemical reaction, R, is described as the rate of consumption of the reactant species or alternately as the rate of appearance of the product species. For a general chemical reaction

$$aA + bB = cC + dD$$

the reaction rate is described mathematically as

$$R = -(1/a)d[A]/dt = -(1/b)d[B]/dt = (1/c)d[C]/dt = (1/d)d[D]/d$$

The fundamental purpose of chemical kinetics is to find a mathematical relationship between R and the concentrations of all chemical species present. Such a relationship is known as a rate law, and for the above reaction would have the form:

$$d[A]/dt = k[A]^w[B]^x[C]^y[D]^z$$

where k, w, x, y and z are experimentally determined constants, and k is known as the rate constant. The reaction is described as being w-th order in the reactant A and as y-th order in product C.

Usually the rate law for a chemical reaction will not be related in a simple way to the concentrations of the reactants. This is because the reaction is composed of a series of simpler steps known as elementary reactions. The rate law of the overall reaction is thus a combination of the rate laws of the elementary reactions. Rate laws of elementary reactions are defined as the product of the concentrations of the reacting species raised to the power of their respective stoichiometric coefficients. The sequence of elementary reactions which comprise the overall reaction is known as the reaction mechanism.

Three basic types of elementary reactions are defined in terms of the number of molecules of reactants which occur in the reaction. These reactions are unimolecular, involving one molecule, bimolecular, involving two molecules and termolecular, involving three reacting molecules. The order of an elementary reaction is simply the sum of the number of reacting molecules; i.e. a bimolecular reaction would be of the second order. Since elementary reactions occur by the collision of the reacting molecules with each other, the probability of higher order reactions is very small. Hence all reactions can be described as sequences of these three basic types of elementary reactions.

Generally one elementary reaction will occur at a rate which is much slower than the other reactions. The rate of the overall reaction will therefore be determined to a large extent by the rate of this slow elementary reaction. The slow elementary reaction is called the rate determining step.

Reaction rates are known to depend on temperature; higher temperatures result in higher reaction rates. The temperature dependence of reaction rates is described by an Arrhenius relationship, which relates the rate constant to the absolute temperature:

$$k = A \exp(-E_a/RT)$$

where A is known as the pre-exponential factor, E_a is the activation energy of the reaction, R is the gas constant and T is the absolute temperature (K). This relationship shows that by calculating the logarithm of the rate constant at several different temperatures, the activation energy, which is a constant dependent on the process, can be determined.

The nature of the reaction mechanism and the activation energy were examined by Glasstone et al. (1941) and resulted in the formulation of transition state theory. This theory explains the transition from reactant molecules to products through the formation and decay of an activated complex. In order to form the activated complex, the reacting species must acquire a sufficient amount of kinetic energy to overcome the activation energy barrier. Once the activated complex has formed, it may decay to the products or may revert back to the reactants. Thus the reaction rate is given by the concentration of activated complexes multiplied by the frequency at which they decay to the products (Glasstone et al., 1941; Lasaga, 1981). It is obvious that at higher temperatures, more of the reactant will react to form an activated complex, and that more activated complexes will decay into the product species.

Previous silicate dissolution studies

The first quantitative study of silicate mineral dissolution was undertaken by Correns and Von Engelhardt (1938). They studied the dissolution of powdered albite in aqueous solutions and found that the release of Na and Si obeyed a rate law with a square root dependence on time. To account for this time dependence, Correns and Von Engelhardt hypothesized that a precipitate formed on the surfaces of dissolving feldspar grains and that the Na and Si had to diffuse through this layer to solution. As the thickness of this layer increased, the rate of diffusion decreased, resulting in a square root dependence on time.

This theory has been further discussed and modified for feldspars by Wollast (1967), Helgeson (1971), Busenberg and Clemency (1976) and for magnesium silicates by Luce et al. (1972). Wollast (1967) proposed that the concentration of Si in solution changed with time according to a rate law which involved diffusion through a precipitate layer and also consumption of Si by precipitation of a hydrous aluminosilicate phase. Wollast was able to demonstrate that his theoretically derived rate law could be easily fitted to his experimental results. Helgeson (1971) argued that while the rate of diffusion of Si through a precipitate layer was the rate controlling process, the actual concentration of Si in solution could be modelled by a series of precipitation reactions. Luce et al. (1972) studied the dissolution of the Mg-silicate minerals forsterite, enstatite and serpentine in distilled water. They found that the dissolution of these minerals involved two distinct phases, a rapid ion exchange at the surface followed by dissolution which obeyed a $t^{1/2}$ rate law. They concluded that the $t^{1/2}$ rate law could be explained by either nonsteady state diffusion within the mineral, or steady state diffusion through a leached surface layer. Busenberg and Clemency (1976) studied the dissolution of several compositions of plagioclase feldspar in distilled water. They found that the dissolution took place in three distinct stages. The first stage occurred very rapidly and was thought to represent the exchange reaction of surface cations with H^+. The second stage was the familiar parabolic kinetics in which the dissolution followed a rate law dependent on $t^{1/2}$. However, in the third stage, Busenberg and Clemency (1976) found that linear kinetics, with the dissolution rate independent of time, replaced the parabolic kinetics. They explained this change in rate laws by assuming that a steady state condition had been attained, in which the rate of formation of the leached layer was exactly matched by its rate of dissolution. Thus steady state diffusion of components through this layer would yield linear kinetics. Paces (1973) proposed that diffusion through a leached layer could result in parabolic kinetics.

However, another possible explanation of silicate dissolution kinetics was being developed at this time. Lagache (1976) postulated that a surface reaction and not solid state diffusion would control the dissolution of silicates. A surface reaction would tend to show linear kinetics, in which the rate of reaction is independent of time. Petrovich (1976) showed theoretically that diffusion through a precipitate phase could not be the rate controlling step in the dissolution of feldspars. Experiments by Holdren and Berner (1978) seem to indicate that a surface reaction instead of diffusion was the most likely rate controlling step in dissolution. Using SEM and X-ray photoelectron spectroscopy, Holdren and Berner (1978) could not find any evidence of a significant thickness of precipitate or leached layer. They also performed experiments in which they treated powdered feldspar with a HF-H_2SO_4 solution before experimentation. They found that the treated feldspar showed only linear kinetics while untreated feldspar showed parabolic kinetics. Holdren and Berner (1978) concluded that a surface reaction was responsible for the observed kinetics of silicate dissolution, and that parabolic kinetics resulted because of the preferential dissolution of ultra-fine particles and disrupted surface sites. The surface reaction hypothesis has been theoretically supported by the work of Dibble and Tiller (1981), Aagaard and Helgeson (1977) and Helgeson _et al._ (1985).Thus it would seem that the dissolution kinetics of silicates are controlled by a reaction that occurs at the surfaces of dissolving grains and not by the diffusion of components through an altered surface layer or precipitate as had been previously proposed. However, two important questions remain to be answered; first, what is the nature of the surface reaction; second, if dissolution occurs by a surface reaction how does this account for the incongruent nature of silicate dissolution. Incongruent dissolution would seem to imply that some sort of surface layer exists, although a layer of significant thickness has yet to be observed. Holdren and Berner (1978) found a leached layer of only a few angstroms thickness in grains of feldspar leached in pH-buffered solutions. The

Table 3. Composition of natural sodalite used in the dissolution experiments.

Oxide	Analysis (wt, %)	Theoretical (wt. %)
Na_2O	25.12	25.6
Al_2O_3	31.17	31.56
SiO_2	36.34	37.19
Cl	7.04	7.32
K_2O	0.23	———
CaO	0.10	———

Analysis carried out by wavelength dispersive electron microprobe analysis. Data reduced by the Bence-Albee method. Analyst: T. Dunn.

present study will address these two questions.

Sample Preparation

A sample of natural sodalite was acquired and analyzed by X-ray powder diffraction and electron microprobe. The X-ray diffraction data were compared against data for natural sodalite in the JCPDS powder diffraction file, and found to be identical within error. No other phases were detected. The composition of the sodalite was determined by wavelength dispersive electron microprobe analysis. The analysis, presented in Table 3, is within 0.5% of the ideal sodalite composition for each element. Apart from minor amounts of K and Ca (< 0.5 wt %), no other impurities were found.

The sodalite was cut into wafers of regular geometric shape (e.g. quadrilaterals, triangles) with a Buehler Micromet saw. All wafer surfaces were ground and polished to 1 um grit. Polishing the wafer surfaces reduced the effect of varying surface roughness between wafers. In addition, polishing produced a smooth surface for SEM and secondary ion mass spectrometry (SIMS) analysis.

The surface area of each wafer was calculated by approximation to a regular geometric shape and measuring the dimensions required by the specific area formula. These dimensions were measured with a micrometer stage petrographic microscope and a hand-held micrometer. Dimensions measured on the micrometer stage are accurate to ±0.1 cm, while dimensions measured with the hand-held micrometer are accurate to ±0.05 cm. These accuracies result in an error of 1-2% in the calculated areas. However, the actual surface areas are greater than the calculated areas because the wafer surfaces have some relief on a microscopic scale. Since it was not possible to directly measure the surface roughness, a 5% error in calculated surface area was adopted for each wafer.

Before beginning an experiment, each wafer was ultrasonically cleaned in acetone to remove any adhering material. The mass of each wafer was then determined on a Mettler balance to an accuracy of ±0.00001g.

Experimental Method

All experiments were conducted in sealed Teflon jars contained in a constant temperature oven set to $50 \pm 1^{\circ}C$. All Teflon jars were rinsed with dilute nitric acid and distilled water prior to use. Each wafer was completely submerged in sufficient leaching solution to yield a surface area to volume ratio of $0.1\ cm^{-1}$. The wafers were mounted across fine platinum wires suspended by the frame of a plastic support. It is estimated that this support exposed more than 99% of the wafer surface area to the leaching solution. A very small fraction of the surface of each wafer was covered by the wire supports.

Four different sets of dissolution experiments were conducted on natural sodalite, to test the effect of pH and

Table 4. Chemical compositions of synthetic brines.

	B300	B500	B700
Ca^{+2}	500	4400	18250
Na^{+}	500	4400	10300
Mg^{+2}	15	50	270
K^{+}	—	14	48
Sr^{+2}	5	44	182
Cl^{-}	1599	14594	48840
SO_4^{-2}	15	88	364
HCO_3^{-}	150	175	74
NO_3^{-}	10	2	5
SiO_2	23	27	55

All concentrations in parts per million.

solution composition on the rate of dissolution. All experiments were conducted at a temperature of 50°C and a pressure of 1 atm. The four types of experiments were:

1) Distilled water experiments, conducted with two separate aliquots of distilled water, pH 6.5 and 7.5. Durations of from 0.5 to 218 days.
2) Distilled water with the initial pH adjusted to predetermined values with HNO_3 or KOH before experimentation: pH 2, 4, 6, 8, 10 and 11. Experimental duration of 20 days. The final solution pH was recorded for each experiment.
3) Buffered pH experiments. Solutions of K-bipthalate, KOH and H_3BO_3 were prepared and used after the method described in Wollast (1967) to produce buffered solutions of pH 6 and 8. Blanks of the solutions were also run to determine the initial concentration of Na Al, Si and Cl. Durations of from 1 to 20 days.
4) Synthetic brine experiments. Brine compositions (see Table 4) were prepared by Atomic Energy of Canada Ltd. Durations of 30 to 90 days.

At the end of each experiment, the wafer was removed from the solution, rinsed with distilled water and dried for at least 24 hours at 110°C prior to re-weighing. All solutions, except the synthetic brines, were analyzed for Na, Al and Si by atomic absorption spectrophotometry and for Cl by specific ion electrode. Details of the analytical method can be found in Appendix 2.

Selected wafers were examined by SEM and submitted to Atomic Energy of Canada Ltd. for secondary ion mass spectrometry (SIMS). The SIMS technique was used to estimate the composition of the surface and near surface region of leached natural sodalite samples. The surface of each sample was bombarded with Ar ions, which caused ionized fragments to be sputtered off. These sputtered fragments were then analyzed by mass spectrometry to provide an estimate of the concentration of elements at the sputtered surface. Since the sputtering gradually exposes greater depths beneath the surface, SIMS provides a method for investigating the variation in composition with depth. Details of this technique are discussed later.

Results

All solution analyses have been recast into a normalized concentration variable with units of moles cm^{-2}. This normalization reduces the effect of varying surface area when the results are compared. The results will be described according to the categories set forth in the previous section.

1. Distilled water experiments.

The distilled water experiments were conducted to establish a baseline for the dissolution of natural sodalite. Since distilled water contains low concentrations of dissolved species, the results obtained can be used to determine the effects of varying solution composition on dissolution.

The solution analyses are presented in normalized form in Table 5 and shown graphically in Figures 5 and 6. Figure 5 shows the results for the pH 6.5 distilled water experiments while Figure 6 shows the results of the pH 7.5 distilled water experiments. There is a considerable amount of variation in the results, which is probably due to undetermined errors in the calculated surface areas. However, two types of trends are noticable in the data. The first trend involves the release of Na and Cl. These elements exhibit high initial release rates in the first ten days of leaching, followed by a decline to lower rates thereafter. The second type of trend involves Si and Al. These elements exhibit constant release rates in all experiments. This suggests that the process which controls the release of Na and Cl may be different than the process controlling the release of Si and Al. The dissolution of natural sodalite was also accompanied by a change in the pH of the distilled water toward a value in the range 7.5 to 8.

A series of SEM images was obtained for several wafers leached in the pH 7.5 distilled water for durations of from 0.5 to 15 days. These images, shown in Plate 2, form a time series illustrating the progressive alteration of the wafer surfaces.

Table 5. Solution analyses of distilled water experiments

Number	Duration (sec.)	R_{Na} $x10^6$	R_{Al} $x10^7$	R_{Si} $x10^6$	R_{Cl} $x10^6$
1	2659392	2.3	2.19	1.92	0.39
2	5176800	2.56	3.26	1.94	0.56
3	613440	2.28	2.93	0.94	——
4	1036800	1.64	4.16	1.56	1.0
5	18835200	1.86	1.75	2.48	0.77
6	14954400	1.68	n.d.	1.6	0.21
7	9763200	2.0	n.d.	1.73	——
8	2174904	0.8	1.19	0.54	0.56
9	2147904	1.42	1.89	0.6	0.56
10	344400	0.52	0.11	1.36	0.72
11	344400	0.51	0.8	0.16	2.2
12	5179766	1.36	n.d.	0.8	5.3
13	10964333	2.13	——	——	3.21
14	10964333	2.02	——	——	2.79
15	7847712	1.83	3.63	1.57	2.03
16	7847712	2.03	4.78	1.60	2.27
17	4058208	3.0	2.2	1.33	2.25
18	4058208	2.16	n.d.	0.67	——

Table 5 continued.

Number	Duration (sec.)	R_{Na} $x10^6$	R_{Al} $x10^7$	R_{Si} $x10^6$	R_{Cl} $x10^6$
19	1374624	1.85	2.93	0.55	1.91
20	1374624	1.69	1.82	0.76	2.27
21	609984	1.76	1.45	0.49	2.67
22	609984	1.26	n.d.	n.d.	2.08
23	173664	1.02	1.42	n.d.	1.61
24	173664	1.03	1.51	n.d.	2.10
25	87264	0.37	1.52	n.d.	1.52
26	87264	0.37	1.35	n.d.	1.66
27	33005	0.11	n.d.	n.d.	1.07
28	33005	0.11	n.d.	n.d.	1.3

The variable R represents the amount of each element released to solution per unit surface area of sample; units moles cm^{-2}.

All experiments performed in sealed Teflon containers maintained at 50°C for the duration of the experiment.

Figure 5. Results of the first series of natural sodalite dissolution experiments in distilled water. The solutions were analyzed for Na, Al and Si by atomic absorption and for Cl by specific ion electrode. All solution analyses have been cast into the normalized variable R, with units of moles cm^{-2}. The horizontal axis shows experimental duration in days. The results for Na are in (a), for Al in (b), for Si in (c) and for Cl in (d).

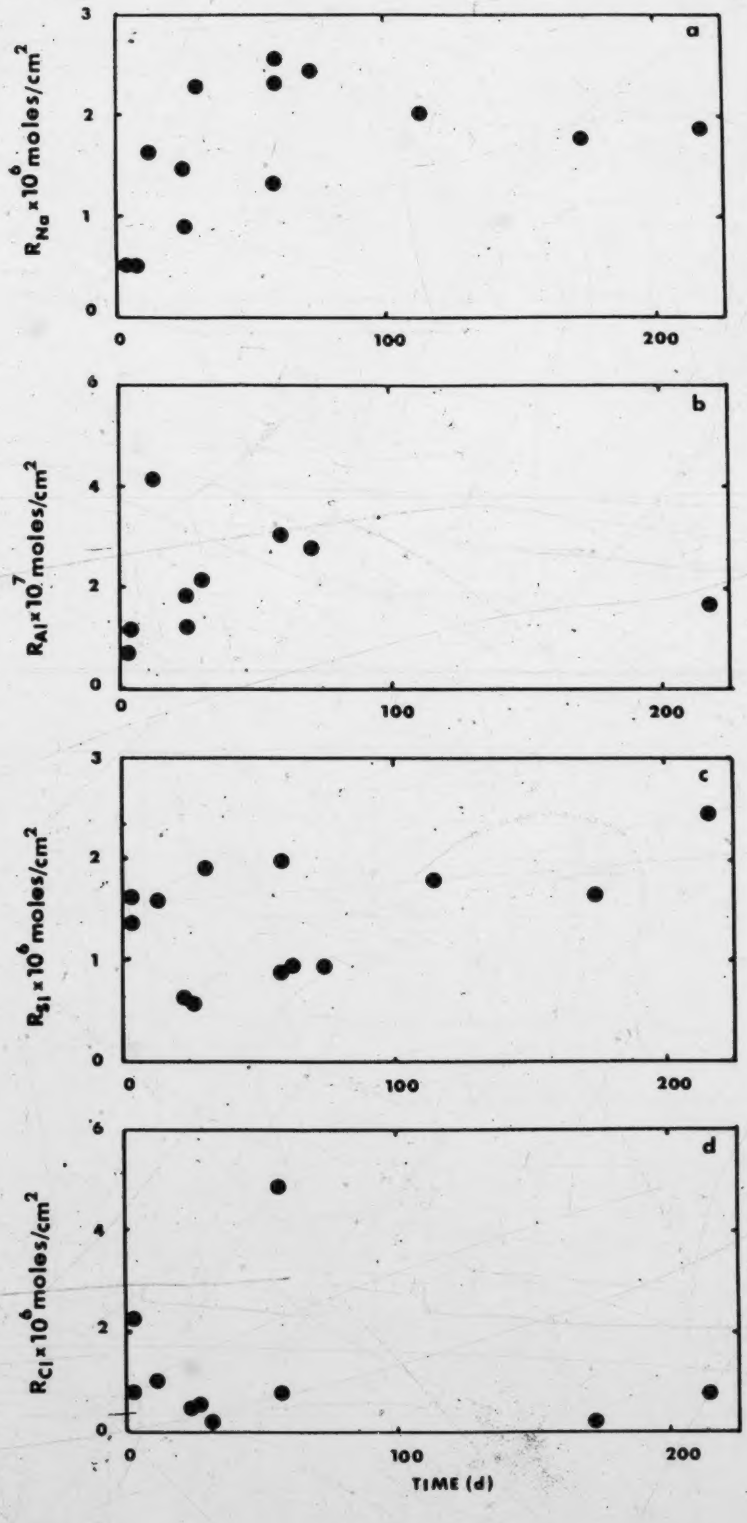
a
$R_{Na} \times 10^6$ moles/cm^2
0
1
2
3
0
100
200
b
$R_{Al} \times 10^7$ moles/cm^2
0
2
4
6
0
100
200
c
$R_{Si} \times 10^6$ moles/cm^2
0
1
2
3
0
100
200
d
$R_{Cl} \times 10^6$ moles/cm^2
0
2
4
6
0
100
200
TIME (d)

Figure 6. Results of the second set of distilled water dissolution experiments on natural sodalite. The solutions were analyzed for Na, Al and Si by atomic absorption spectroscopy and for Cl by specific ion electrode. The results of the solution analyses have been recast into a normalized form with units of moles cm^{-2}. The horizontal axis shows experimental duration in days. The results for Na are in (a), for Al in (b), for Si in (c) and for Cl in (d).

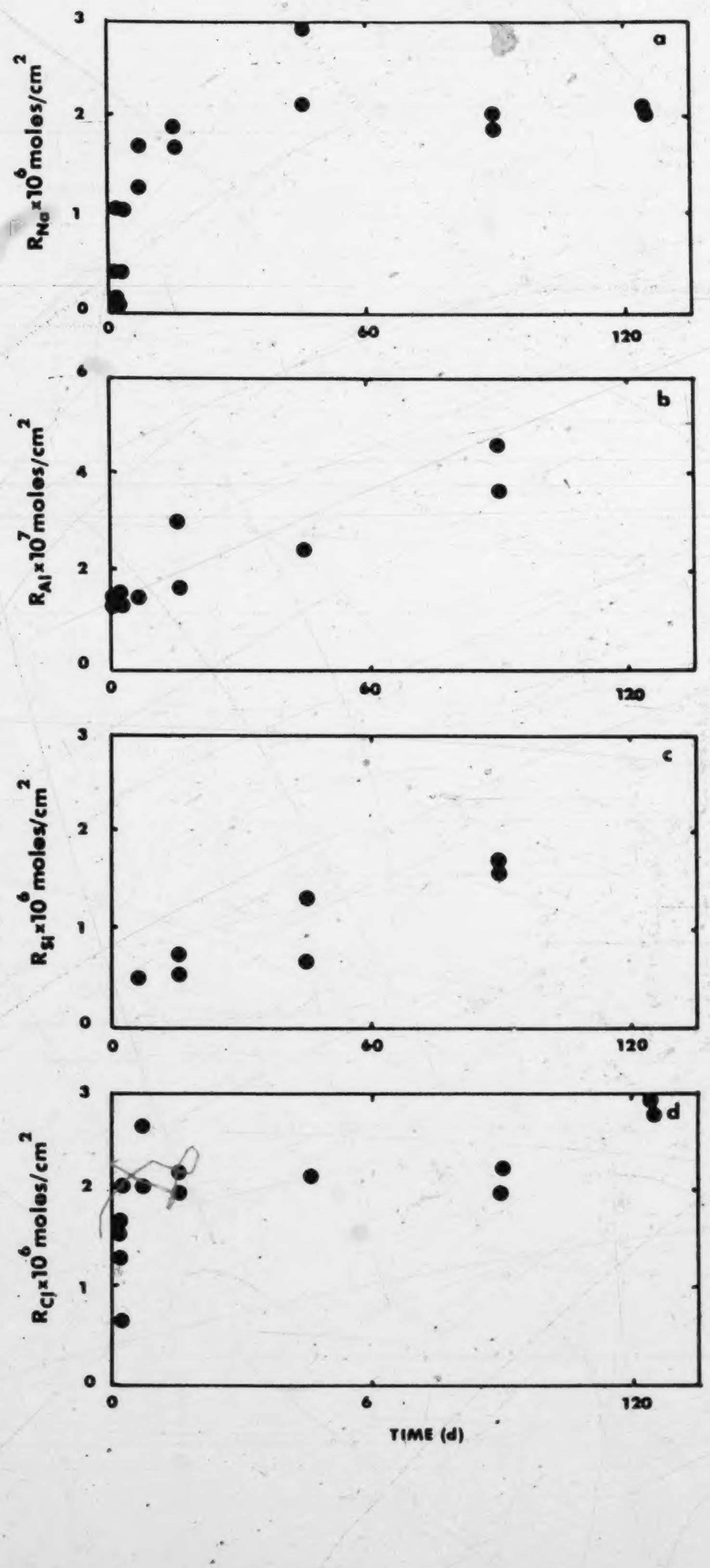
a
$R_{Na} \times 10^6$ moles/cm^2
0
1
2
3
0
60
120
b
$R_{Al} \times 10^7$ moles/cm^2
0
2
4
6
0
60
120
c
$R_{Si} \times 10^6$ moles/cm^2
0
1
2
3
0
60
120
d
$R_{Cl} \times 10^6$ moles/cm^2
0
1
2
3
0
6
120
TIME (d)

Plate 2. Scanning electron microscope photomicrographs of natural sodalite wafer surfaces leached in distilled water. A range of leaching times is represented by the photomicrographs:

(a) unleached surface.
(b) surface leached for 0.5 day
(c) surface leached for 1 day
(d) surface leached for 2 days
(e) surface leached for 7 days
(f) surface leached for 15 days
(g) surface leached for 15 days

All photomicrographs except for (g) show a scale bar of 10 um length. Photograph (g) shows a larger area of the surface of (f) and has a scale bar of 40 um length.

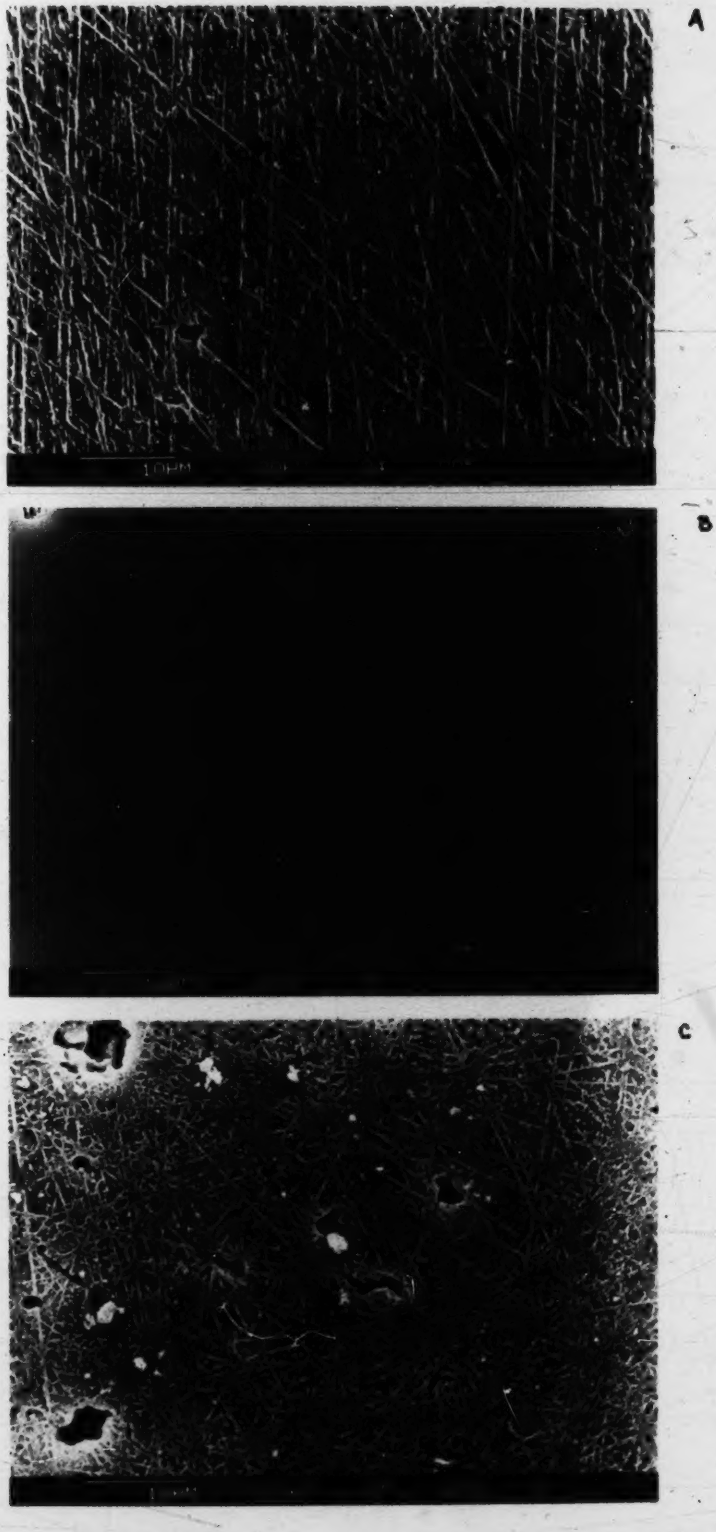
A
10µm
B
C

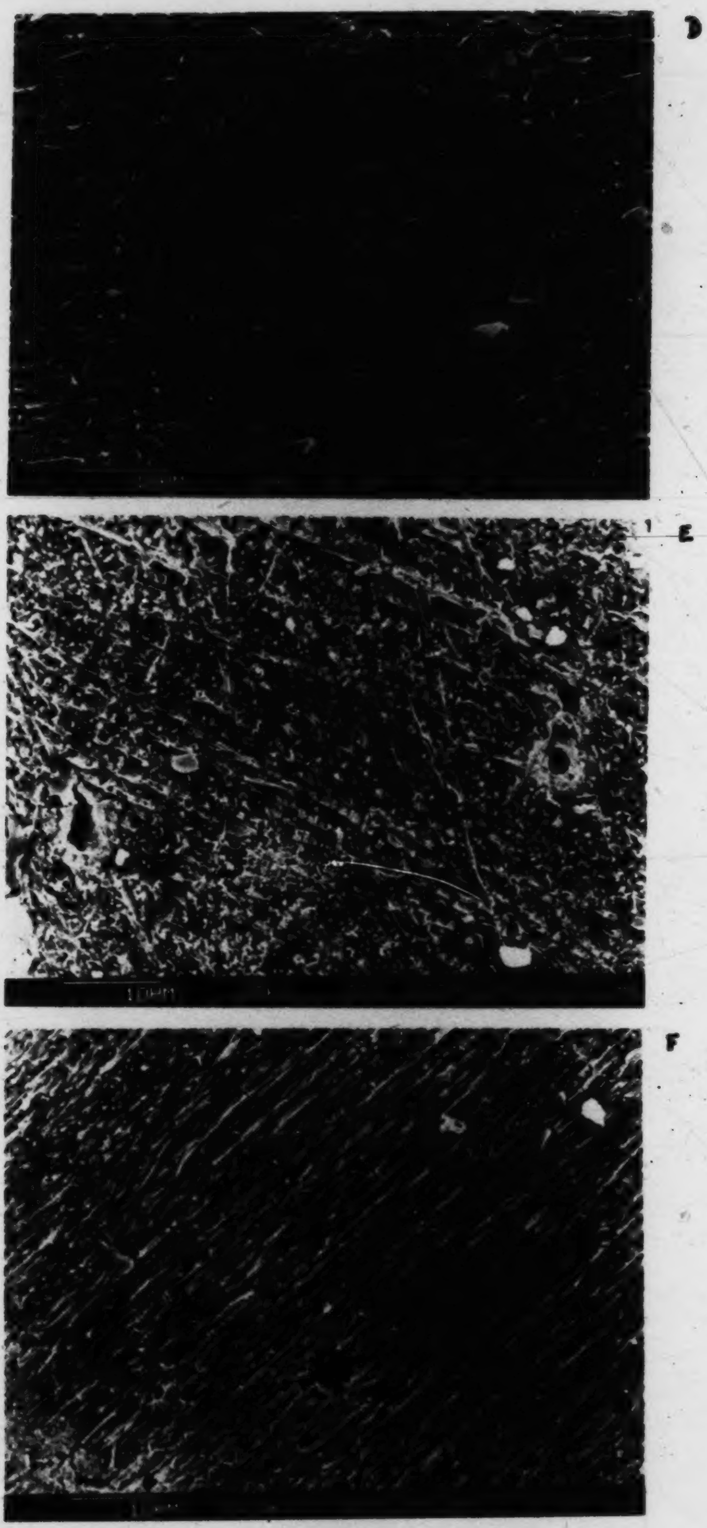
D
E
10µm
F

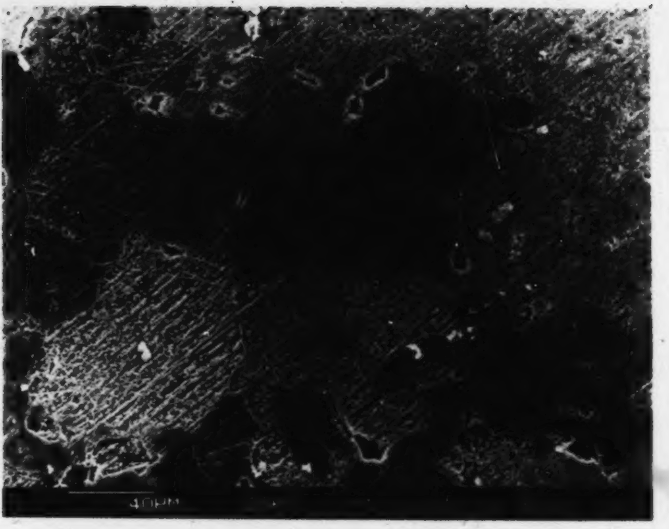
40μm
G

All wafers were highly polished before the beginning of each experiment. The wafer surfaces were rapidly etched in the first 10 to 15 days followed by very slow change thereafter, a pattern which was also observed in the Na and Cl release rates, which implies that the rate of Na and Cl release is strongly related to the rate of surface alteration.

The SEM images also indicate a discrepancy between the geometric and actual surface areas. The actual surface area will become increasingly etched. This etching was also visible to the naked eye as a tarnishing of the surface. Significant etching has occurred after only 0.5 day (Plate 2a). The etch patterns change from apparently random orientations to a regular arrangement of pits and ridges. The early etch patterns are quite similar to scratches produced during early stages of wafer grinding and polishing. This suggests that initial dissolution occurs along the remnants of scratches on the surface. The wafer surface shown in Plate 2e was produced after 15 days in distilled water and has a fibrous appearance. This texture is very similar to that found on a wafer which had been leached for 30 days in pH 6.5 distilled water. This implies that the surface is altered very quickly within the first 10 to 15 days, and changes only very slowly afterwards. This pattern of rapid change is thought to be dependent on the roughness of the surface (Helgeson and Aagaard, 1984). It is apparent that the surface roughness increases with time, which means that the actual surface area also increases with time. ever Plate 2f, showing the surface of natural sodalite leach for 15 days in pH 7.5 distilled water, shows three distinct areas with different degrees of roughness. Thus the actual surface area not only increases with time, but it also apparently increases in a random and uneven fashion. The error in calculated surface area is therefore not a smooth function of time and a correction cannot be applied to the calculated surface areas.

The solution data can be treated statistically to derive empirical reaction rate laws. Since it is apparent that the analyses from the distilled water with an initial pH of 7.5 display less variation than the analyses from the pH 6.5 distilled water, these data will be used to determine the rate laws.

The Si and Al data can be treated simply with a zeroth order rate law. The normalized solution concentration, R, is a simple function of time. The integrated rate law is of the form

$$R_i = K_i t \qquad (1)$$

where the R_i refers to the normalized concentration of Si or Al, K_i refers to the empirical rate constant for Si or Al, and t refers to the experimental duration in seconds. Equation (1) is linear with respect to time. Therefore the data can be subjected to linear regression, with R_i regressed against t. Table 6 shows the results of the linear regressions for Si and Al. Given the amount of random variation present in the data,

Table 6. Regression analysis of the distilled water experimental data.

1. Na

$R = a + bt$		$R = a + b\ln t$
$t < 10$ days	$t > 10$ days	
$a = 2.6 \times 10^{-7}$	$a = 1.8 \times 10^{-6}$	$a = -3.3 \times 10^{-6}$
$b = 2.2 \times 10^{-12}$	$b = 2.4 \times 10^{-14}$	$b = 3.4 \times 10^{-7}$
$r^2 = 0.78$	$r^2 = 0.32$	$r^2 = 0.9$

2. Al

$R = a + bt$

$a = 1.3 \times 10^{-7}$

$b = 3.5 \times 10^{-14}$

$r^2 = 0.91$

3. Si

$R = a + bt$

$a = 4.8 \times 10^{-7}$

$b = 1.5 \times 10^{-13}$

$r^2 = 0.92$

4. Cl

$R = a + bt$		$R = a + b\ln t$
$t < 10$ days	$t > 10$ days	
$a = 1.3 \times 10^{-6}$	$a = 1.9 \times 10^{-6}$	$a = -1.0 \times 10^{-6}$
$b = 1.8 \times 10^{-12}$	$b = 8.1 \times 10^{-14}$	$b = 2.2 \times 10^{-7}$
$r^2 = 0.71$	$r^2 = 0.53$	$r^2 = 0.74$

these regressions fit the experimental data quite well.

The Na and Cl data show significant non-linear behavior with respect to time. A simple linear expression will not suffice to describe these data. Inspection of Figures 6a (Na) and 6d (Cl) suggests that a rate law of the form

$$R_i = K_i \ln (t) \qquad (2)$$

can be fitted to the data. As before, R_i refers to the normalized concentration of Na or Cl, K_i is the rate constant for Na or Cl, and ln (t) is the natural logarithm of the experimental duration in seconds. This equation is linear with respect to ln (t) and linear regression may be applied, regressing R_i against ln (t). The results of the linear regressions for Na and Cl are presented in Table 6. The negative intercepts are not physically meaningful and can be interpreted as zero. These empirical rate laws fit the experimental data closely and reproduce the elemental release curves accurately.

Thus it is concluded that the rates of release of Na and Cl are very time dependent and non-linear in these experiments, while the release rates of Si and Al are independent of time. Since these experiments were not conducted with any control on pH, any interpretation of the difference in the rate laws of Na and Cl versus Si and Al must take into account the change in solution pH with time. Therefore the effect of solution pH on dissolution rates must be determined.

2. Initial pH experiments.

The distilled water experiments indicated that solution pH may have a significant effect on rates of dissolution. The initial pH experiments were conducted to study two aspects of the pH control on sodalite dissolution: 1) the effect of initial pH on dissolution and, 2) how the final solution pH changes as a function of the initial pH.

The experimental results are given in Table 7 in normalized form and shown graphically in Figure 7. The effect of initial pH is immediately obvious from Figure 7. There is over an order of magnitude difference in the amount of dissolution between the pH 2 and the pH 8 results. In addition there is a minimum in the amount of dissolution, occurring at a pH of approximately 8. This minimum of dissolution is also recorded by the pH change, which is smallest at pH 8. The direction of the pH change is always toward 8 no matter what the initial value. Thus the dissolution of sodalite tends to buffer the solution pH at a value of approximately 8.

3. Buffered pH experiments.

The previous experiments have demonstrated the importance of solution pH in controlling the rate of sodalite dissolution. However, the previous experiments were carried out in such a way that the pH was allowed to change. The interpretation of these results is difficult since no quantitative information about the time dependence of pH was obtained. The buffered pH experiments

Table 7. Solution analyses of the initial pH experiments

Number	pH_i	pH_f	R_{Na} x10^6	R_{Al} x10^6	R_{Si} x10^6	R_{Cl} x10^6
1	2.00	3.84	83.4	169	121	48.5
2	2.00	3.76	187	128	140	58.3
3	4.00	5.61	2.3	2.8	3.4	5.3
4	4.00	5.36	7.8	4.9	5.6	7.2
5	6.00	6.70	2.3	.62	1.1	3.4
6	6.00	6.48	2.3	8.0	1.9	3.3
7	8.00	8.03	5.3	1.5	2.6	3.2
8	8.00	7.9	3.0	0.5	1.7	2.3
9	10.00	9.54	5.4	3.9	3.0	1.1
10	10.00	9.28	3.8	2.4	1.4	7.2
11	11.00	10.72	2.3	8.6	6.1	2.1

pH_i refers to the initial pH at the beginning of the experiment while pH_f refers to the pH of the solution after the experiment.

R is the normalized solution analysis variable, with units of moles cm^{-2}.

Figure 7. Solution analyses for the initial pH experiments. All analyses have been normalized to unit surface area. The common logarithms of the solution analyses have been plotted in order to allow all analyses for one element to fit on the same figure. The Na analyses are in (a), Al in (b), Si in (c) and Cl in (d). Figure 7e. shows the change in pH versus the initial solution pH.

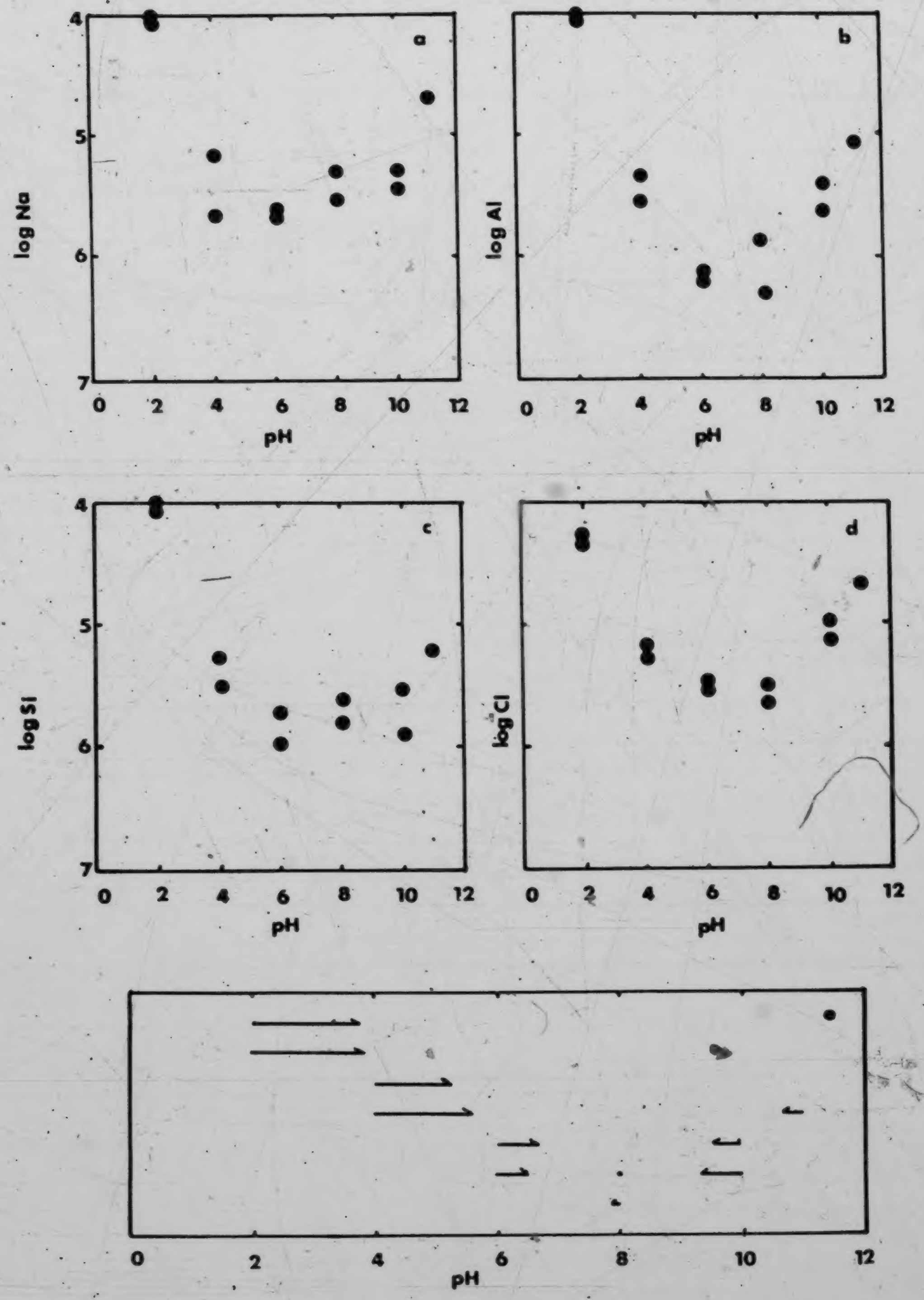
a
log Na
4
5
6
7
0
2
4
6
8
10
12
pH
b
log Al
0
2
4
6
8
10
12
pH
c
log Si
4
5
6
7
0
2
4
6
8
10
12
pH
d
log Cl
0
2
4
6
8
10
12
pH
0
2
4
6
8
10
12
pH

Table 8. Solution analyses of the buffered pH experiments

pH 6.0 experiments

Number	Duration (sec.)	R_{Na} x10^6	R_{Al} x10^7	R_{Si} x10^6	R_{Cl} x10^6
1	75600	2.04	0.74	1.42	0.55
2	75600	2.01	0.75	1.23	0.57
3	179712	0.82	0.34	0.96	0.32
4	179712	2.13	0.76	1.49	0.64
5	437184	5.09	0.87	3.84	1.79
6	437184	6.93	1.34	6.02	3.09
7	880416	9.61	0.91	8.67	7.3
8	880416	12.3	0.97	9.78	5.15
9	1369824	16.5	0.72	9.58	3.94
10	1369824	14.9	0.89	7.46	3.77
11	2002752	6.65	0.96	4.97	1.93
pH 8.0 experiments					
1	275616	1.0	0.63	0.76	0.62
2	275616	0.93	0.52	0.76	0.41
3	519264	1.31	——	——	0.7
4	519264	1.32	——	——	0.59
5	930528	1.92	1.63	1.54	0.9
6	930528	1.74	1.29	1.19	0.7
7	1283040	1.82	1.59	1.85	1.35
8	1283040	1.31	0.79	1.23	0.99

were conducted to eliminate the pH variation and to determine the pH independent dissolution rates of natural sodalite.

The results are listed in Table 8 and shown in Figure 8. Both sets of pH experiments are shown in each diagram for easy comparison. The effect of buffered pH on sodalite dissolution is immediately obvious from Figure 8. Except for Al, the normalized concentrations fall along two linear trends which are dependent upon the solution pH.

It is possible to fit pH-independent rate laws to these data. Na, Si and Cl all obey a rate law of the form

$$R_i = K_i t \qquad (3)$$

where R_i is the normalized solution concentration of Na, Si or Cl, K_i is the empirical rate constant for a given pH and element, and t is the experimental duration in seconds. Linear regression was applied to the data, and the results are listed in Table 9.

The regression analysis shows that the rate of dissolution under pH buffered conditions is constant over time. The rate of dissolution at pH 6.0 is approximately ten times the rate at pH 8.0 for each element. The process of dissolution under pH buffered conditions appears to be somewhat different from the dissolution in distilled water. The surfaces of wafers leached in the buffer solutions are not noticably altered. Instead, dissolution occurs along cracks and fractures in the wafer. The fibrous texture which is apparent on the surfaces of wafers

Figure 8. Solution analyses for the buffered pH dissolution experiments. The analyses have been recast into units of moles cm^{-2}. Two sets of experiments are represented on the diagrams. Circles represent experiments carried out in pH 6.0 buffer, while squares represent experiments carried out in pH 8.0 buffer. The Na analyses are in (a), Al in (b), Si in (c) and Cl in (d).

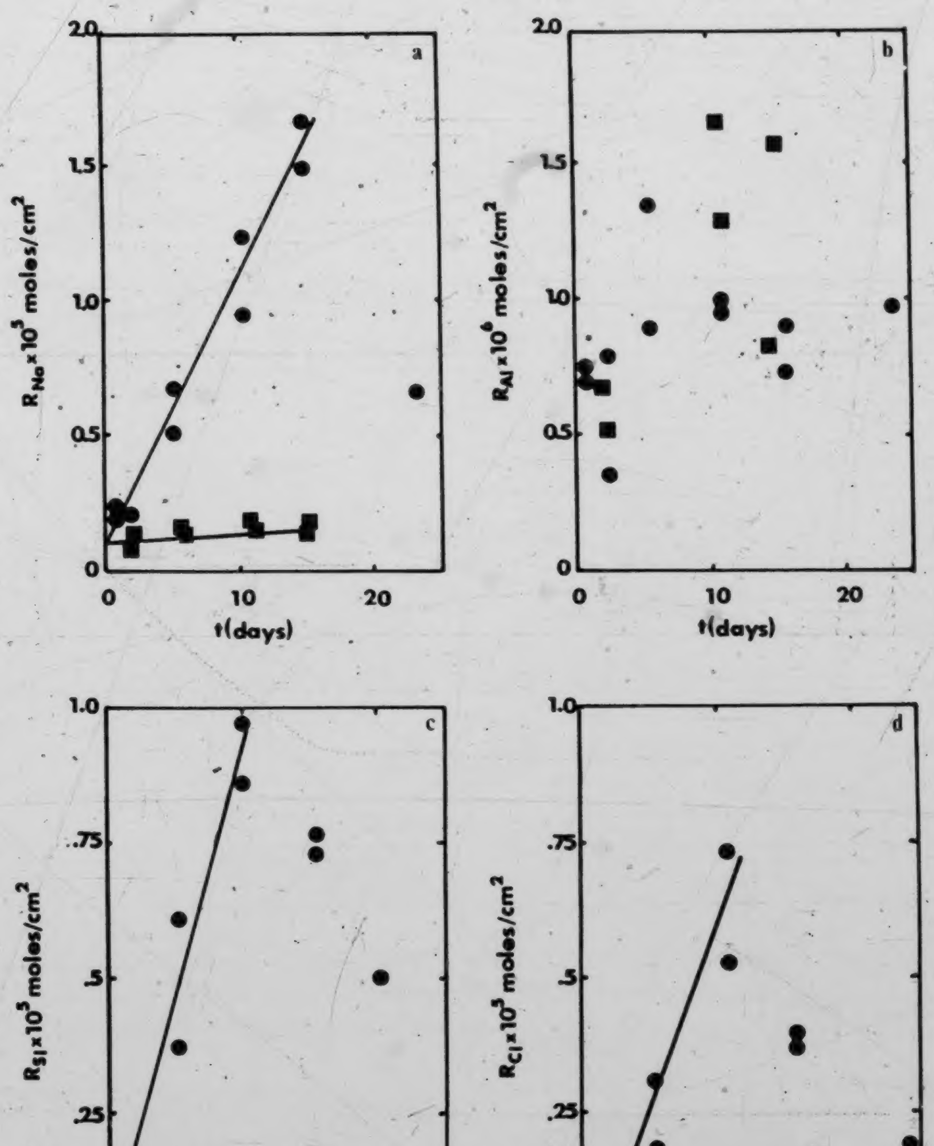
a
$R_{Na} \times 10^3$ moles/cm^2
2.0
1.5
1.0
0.5
0
0
10
20
t(days)
b
$R_{Al} \times 10^6$ moles/cm^2
2.0
1.5
1.0
0.5
0
0
10
20
t(days)
c
$R_{Si} \times 10^3$ moles/cm^2
1.0
.75
.5
.25
0
0
10
20
t(days)
d
$R_{Cl} \times 10^3$ moles/cm^2
1.0
.75
.5
.25
0
0
10
20
t(days)

Table 9. Rate laws for release of Na, Si and Cl in pH buffered solutions.

	pH 6.0	pH 8.0
Na		
	$a = 4.72 \times 10^{-7}$	$a = 9.23 \times 10^{-7}$
	$b = 1.17 \times 10^{-11} t$	$b = 6.6 \times 10^{-13} t$
	$r = 0.98$	$r = 0.73$
Al		
	$a = 7.56 \times 10^{-7}$	$a = 4.9 \times 10^{-7}$
	$b = 1.27 \times 10^{-13} t$	$b = 7.03 \times 10^{-13} t$
	$r = 0.25$	$r = 0.65$
Si		
	$a = 1.31 \times 10^{-6}$	$a = 3.79 \times 10^{-7}$
	$b = 6.31 \times 10^{-12} t$	$b = 9.54 \times 10^{-13} t$
	$r = 0.86$	$r = 0.86$
Cl		
	$a = 5.8 \times 10^{-7}$	$a = 3.41 \times 10^{-7}$
	$b = 3.7 \times 10^{-12} t$	$b = 5.94 \times 10^{-13} t$
	$r = 0.76$	$r = 0.85$

Units: a - moles cm^{-2}; b - moles $cm^{-2}\ s^{-1}$.

leached in distilled water is not present on the surfaces of the wafers leached in the pH buffers.

Synthetic brine experiments

The synthetic brines are modelled after those found in some plutons of the Canadian Shield. Experiments were carried out in these brines to establish a baseline for the effect of concentrated solutions on the dissolution of sodalite.

The solutions could not be analyzed because of the high concentrations of all species present. Thus there are no data on the amount of dissolution that took place during these experiments. However, the surfaces of the wafers were examined by SEM. SEM images of the wafer surfaces are shown in Plate 3. It can be seen that no evidence of large-scale alteration is present. In several cases (e.g. Plate 3c, SCSSS) there is evidence which suggests that a precipitate formed on the surfaces. It should be recognized that the pH of the synthetic brines was approximately 7.5 to 8. In view of the previously observed pH effect on dissolution, this may explain the stability of the wafers in the brine solutions.

SIMS analysis of wafer surfaces

Secondary ion mass spectrometry (SIMS) is a relatively new analytical technique. It permits the chemical analysis of surfaces on a nanometer scale. The instrument is composed of an ion gun which sputters particles from the sample surface, and a

Plate 3. SEM microphotographs of natural sodalite surfaces leached in the synthetic brines:

a. unleached surface

b. leached for 30 days in B300

c. leached for 30 days in B500

d. leached for 30 days in B700

e. leached for 30 days in SCSSS

f. leached for days in

In all cases, a scale bar of 10 or 20 um is shown.

A
C

D

E

F

mass spectrometer which measures the frequency of occurrence of sputtered ions with given masses. These measurements are converted into electronic signals whose intensities are dependent on the corresponding ionic frequencies of occurrence. The primary ions, usually Ar^+ or O^+, gradually sputter away the surface atoms and expose those immediately below the surface. Thus SIMS allows depth profiling of sample composition. Output from the analysis consists of a chart which shows the measured intensities for the various mass species present plotted agains the sputter time, which is proportional to the depth from the original surface.

The basic assumption that underlies SIMS analysis is that the numbers of various mass species measured by the mass spectrometer are proportional to their concentration at the surface of the sample (Brundle, 1982). To relate the observed signal intensities to surface composition, it is necessary to understand the process by which secondary ions are produced. However this process is not well understood at the present time. The incident primary ions undergo many inelastic collisions with the atoms at the surface and immediately underneath the surface. In a complex and poorly understood process, some particles will acquire sufficient energy to break the local bonds and will be ejected from the surface. Of the ejected particles, some will be ionized and can therefore be analyzed by mass spectrometer. Determining how many particles of a given mass species (e.g. Na) will be ionized and recorded by the mass spectrometer is a complex function of the surface chemistry, the efficiency of the sputtering process, the probability that any given particle will be ionized, and constants characteristic of the mass spectrometer (Brundle, 1982; Werner, 1975). Thus to quantify SIMS analyses it is necessary to convert signal intensity to concentration and sputter time to depth. Unfortunately, no satisfactory method has yet been developed to quantify SIMS analysis (Brundle, 1982).

The SIMS instrument used in this study is located at the Whiteshell Nuclear Research Establishment near Pinawa, Manitoba. Argon gas was used as a source of primary ions, which had energies of 4.5 KeV. A simple quantification procedure was adopted for this study. To permit quantification, certain simplifying assumptions were made. Firstly, it was assumed that the signal intensities for all species were directly proportional to the concentrations on the sample surface. Secondly, it was assumed that the rate of sputtering was constant throughout the analysis. These assumptions allow the two conversions mentioned previously (intensity to concentration and sputter time to depth) to be made.

The SIMS analyses were received in the form of charts of signal intensity (counts/sec) versus sputter time. Quantification was carried out for Na, Al, Si and Cl, the principal components of sodalite. The intensity-time profiles for each of these elements were sampled at regular intervals along the time axis. The point where all intensities were greatest and the gradients of all profiles essentially zero was assumed to represent the bulk sodalite composition. These intensities were assumed to represent a definite number of atoms of each element; 4000 Na atoms, 3000 Al atoms, 3000 Si atoms, 1000 Cl atoms and 12000 O atoms. These numbers are in direct stoichiometric proportion to the actual atomic abundances in sodalite. Thus by taking the ratio of the signal intensities at a given time (i.e. distance) to the intensities representative of bulk sodalite composition, the proportions of the different atomic species present can be calculated. It is then a simple matter to convert these calculated atomic proportions to weight percentages of the elements.

This quantification procedure is quite simple and undoubtedly subject to error. It was mentioned previously that there is no simple relationship between the observed intensities and concentrations at the surface. Since the relationship has not yet been quantified (Brundle, 1982), the only reasonable approach is the one adopted here. In addition, the actual rate of sputtering is not well known. Information supplied with the analyses gave the sputtering rate as 2 nm/min, and this value was used for this study. Thus, given the uncertainties in the method, the quantification procedure adopted here is reasonable if its limitations are recognized.

Figure 9. Quantified SIMS profiles of natural sodalite wafers leached in distilled water for varying times. In all figures the vertical axis is wt. % element while the horizontal axis is distance in nanometers from the surface.

a. profile from an unleached sample. Line styles: solid line - Na; dotted line - Cl; dashed line - Al; dot dash line - Si.

b. profile from a sample leached for 30 days. Line styles same as in (a).

c. composite of profiles for Cl, showing unleached (solid line), leached 30 days in distilled water (dot dash line), leached 70 days in distilled water (dashed line) and leached for 120 days in distilled water (dotted line).

d. composite profiles for Na. Line styles as in (c).

e. SIMS profile from a natural sodalite wafer leached for 71 days in SCSSS. Line styles as in (a).

f. SIMS profile from a natural sodalite wafer leached for 30 days in B500. Line styles as in (a).

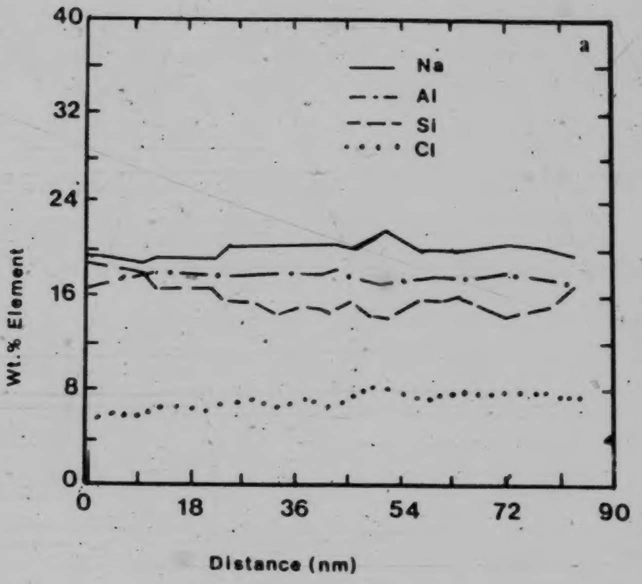
a
Na
Al
Si
Cl
Wt.% Element
0
8
16
24
32
40
0
18
36
54
72
90
Distance (nm)

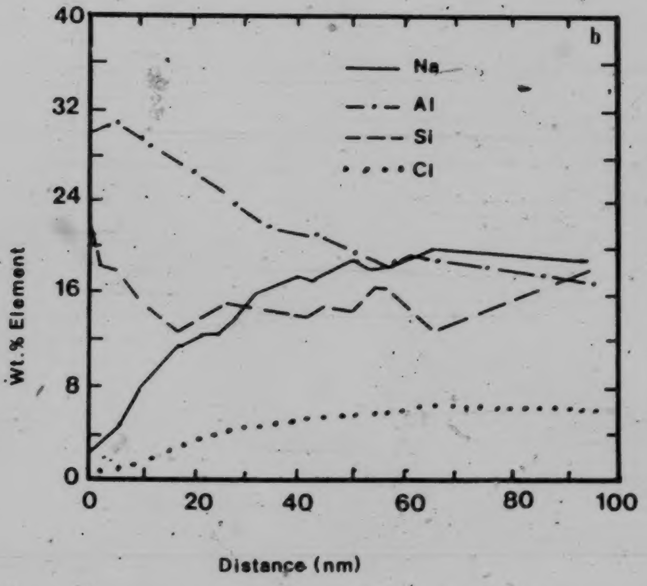
b
Na
Al
Si
Cl
Wt.% Element
0
8
16
24
32
40
0
20
40
60
80
100
Distance (nm)

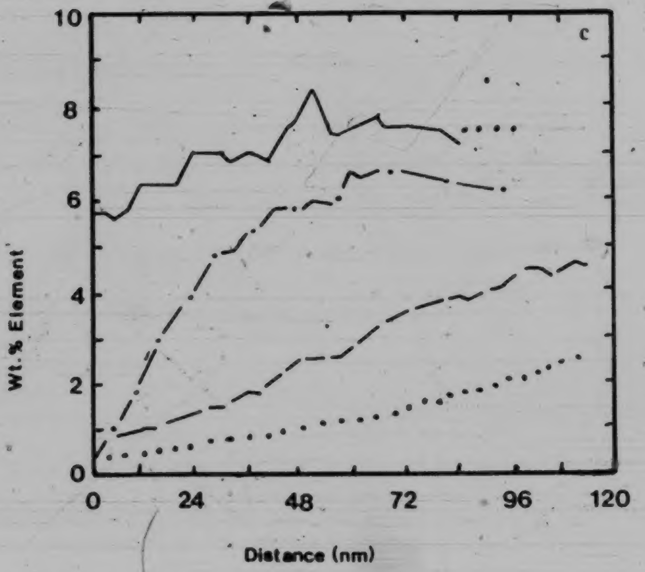
c
Wt.% Element
Distance (nm)
0
2
4
6
8
10
0
24
48
72
96
120

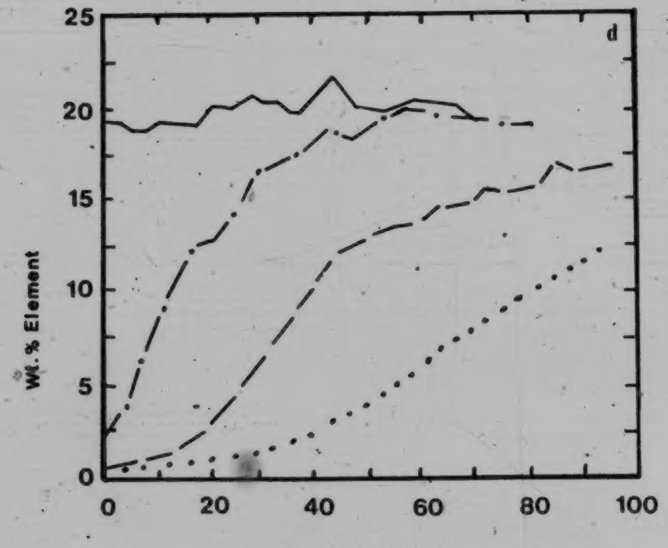
d
Wt.% Element
Distance (nm)
0
5
10
15
20
25
0
20
40
60
80
100

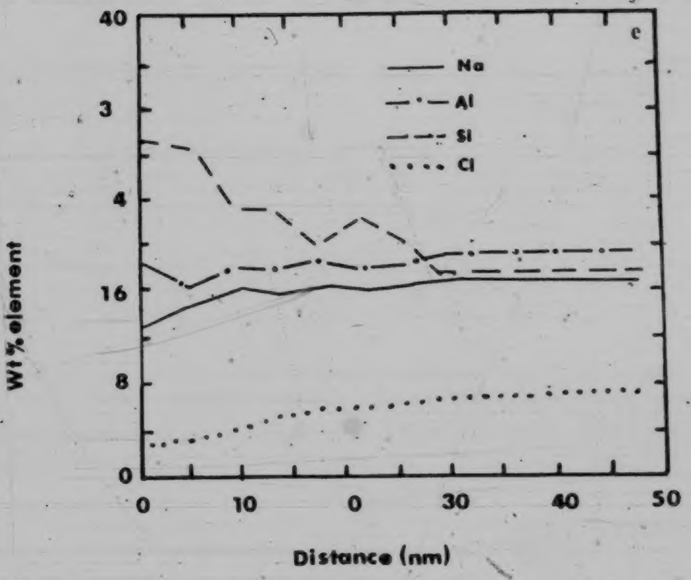
e
Na
Al
Si
Cl
Wt% element
40
3
4
16
8
0
0
10
0
30
40
50
Distance (nm)

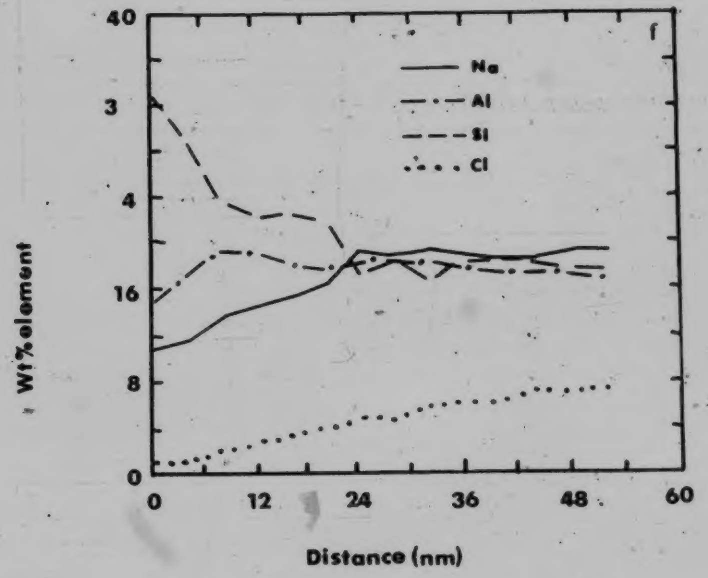
f
Na
Al
Si
Cl
Wt% element
40
3
4
16
8
0
0
12
24
36
48
60
Distance (nm)

Figure 9a shows the quantified SIMS analysis for an unleached wafer while Figure 9b shows the profile for a wafer which was leached for 30 days in distilled wafer. The Na and Cl profiles show a significant depletion with respect to the profiles from the unleached wafer. The Si and Al profiles show an enrichment over the unleached sample. This enrichment is probably a result of the depletion of Na and Cl. Figures 9c and 9d show the Na and Cl profiles for uneached sodalite and sodalite wafers leached for 30, 71 and 113 days in distilled water. The depth of the region depleted in Na and Cl increases with increasing experiment duration. For the 30 day distilled water experiment, the Na profile is approximately 50 nm in length. The equivalent Cl profile is approximately 60 nm in length. In the 113 day experiment, the Na profile is not completely covered by the SIMS analysis, and is thus longer than 120 nm. This is true also of the Cl profile. In each case, it is observed that the Cl profile is longer than the Na profile.

Figures 9e and 9f show the SIMS analyses for the 71 day SCSSS experiment and the B500 experiment. Given the approximations discussed above, it is nevertheless clear that in the 71 day SCSSS experiment a layer which is depleted in Na and Cl and enriched in Si and Al has formed. The Na and Cl profiles are approximately 40 nm long. The Si and Al profiles show slight enrichment, with Si showing a sharp increase near the surface. This enrichment at the surface could be caused by a precipitate of some silicate phase. The SIMS analyses indicate that a surface layer which is depleted in Na and Cl relative to unleached sodalite has formed in all of the experiments. The extent of this depleted layer increases with increasing leaching time. The maximum extent observed was in excess of 120 nm, and occurred in the 113 day distilled water experiment. Wafers that were leached in the artificial brines SCSSS and B500 showed depleted layers which were much less extensive than the wafers leached in distilled water.

Discussion

These dissolution experiments clearly indicate that solution pH is the dominant factor in the dissolution of natural sodalite. Under conditions of constant pH, the rates of release of the constituents of sodalite are constant. This directly supports the hypothesis that a surface reaction controls dissolution. However, the SIMS analyses indicate that a layer leached in Na and Cl exists near the surface of samples. This observation lends support to the hypothesis that diffusion controls dissolution. These hypotheses are apparently mutually exclusive, yet there is evidence to support both. Since both processes cannot be rate-controlling, one or the other must dominate. In the following discussion, an attempt will be made to determine which theory of silicate dissolution best describes the results of this study.

The sodalite dissolution reaction may be written as:

$$2Na_4Al_3Si_3O_{12}Cl + 24H_2O =$$
$$8Na^+ + 6Al(OH)_3 + 6H_4SiO_4 + 2Cl^- + 6OH^-$$

This reaction shows that $6H^+$ ions are consumed and that $3OH^-$ ions are produced in dissolution. This accounts for the observed increase in pH in the distilled water experiments. However, the reaction does not explain the nature of the observed minimum rate of dissolution at a pH of approximately 8.0. The reaction does indicate the importance of H^+ in the reaction, although no indication of the mechanism of dissolution is given.

Experiments have shown that at constant $[H^+]$, the dissolution kinetics of silicate minerals exhibit rate laws of the form:

$$R = k_1 t$$

where R is the rate of dissolution, k_1 is an empirical rate constant and t is time (e.g. Holdren and Berner, 1978). In addition, experiments have also shown that the dissolution rate has a fractional order with respect to the concentration of $[H^+]$. Specifically, the rate law has the form:

$$R = k_2[H^+]^n$$

where R is the rate of dissolution, k_2 is the empirical rate constant, $[H^+]$ is the concentration of H^+, and n is a fractional exponent in the range $0.5 \leq n \leq 1.0$ (Lasaga, 1981). If dissolution is to occur by a surface reaction, then it must be consistent with these empirical rate laws, should explain the minimum in dissolution observed for natural sodalite, and should explain the SIMS results obtained for this study. These considerations will be discussed below.

The nature of the surface reaction has been discussed in detail for feldspars by Aagaard and Helgeson (1982), Lasaga (1981) and Helgeson et al. (1985). To understand the nature of the surface reaction, consideration must be given to the different stages of the reaction. It is generally agreed that silicate minerals dissolve in three distinct steps (Aagaard and Helgeson, 1982):

i) Attachment of H^+ ions by adsorption to specific sites on the dissolving surface.

ii) Exchange of adsorbed H^+ ions and loosely bound surface cations, with the eventual desorption of the exchanged cations.

iii) Decomposition of the protonated aluminosilicate structure, releasing it to solution.

Each of these stages will be examined below.

To understand the process by which H^+ ions become attached to the surface, the nature of the surface must be understood. On a microscopic scale the surface is not a smooth plane, but is instead composed of many discontinuities and irregularities. The presence of these irregularities is very important in the dissolution process. At the surface the continuity of the crystalline structure has been disrupted. As a result there exist partially coordinated cations and anions at the solution-surface interface. These ions give rise to an electrostatic potential gradient in the solution close to the surface. Ions, such as H^+ are attracted to the surface and may become attached or adsorbed, to the surface (Lasaga, 1981). The process of adsorption can be modelled through the application equations known as adsorption isotherms. The basic assumption underlying isotherms is that at a given temperature the number of surface sites available for occupation is in equilibrium with the number of sites already occupied. Lasaga (1981) has shown how the application of a type of isotherm in calculating the release of Na from feldspar can explain the pH dependence of the rate. Previous experimental studies by Grandstaff (1977) and Berner _et al._ (1980) have shown that rates of dissolution are proportional to $[H^+]^n$, where $0.5 \leq n \leq 1.0$. The derivation presented by Lasaga (1981) demonstrates that the fractional order of the dissolution rate law is a direct consequence of the adsorption process. He shows how the rate of Na-H exchange depends on the rate at which H^+ can be adsorbed onto the surface. Adsorption is the physical process by which chemical species, such as H^+ become weakly bonded to a reactive surface by Van der Waals' bonds or intermolecular forces. The feldspar surface has many sub-microscopic irregularities which possess greater surface energies than would a more uniform surface. Removal of these irregularities would therefore result in a greater reduction in the Gibbs free energy of the surface (Lasaga, 1981).

The rate of H^+ adsorption is assumed to be the same as the rate of desorption of exchanging species (e.g. Na^+), and an equilibrium condition exists for the adsorption-desorption reaction. It is therefore possible to describe the equilibrium in terms of an adsorption isotherm, relating the fraction of occupied sites to the fraction of unoccupied sites through a type of equilibrium constant. Lasaga (1981) manipulates this adsorption isotherm and shows that the rate of dissolution, expressed as the rate of Na^+ release does indeed follow an exponential dependence on the concentration of H^+.

This is convincing evidence to support the theory that the rate of silicate dissolution is governed primarily by the concentration of H^+ ions in solution. For a fixed $[H^+]$, Lasaga's derivation suggests that the rate of dissolution is constant. This is in agreement with experimental observations. If it is accepted that the rate of dissolution is dependent only on the $[H^+]$, then the form of the rate laws for Na release from natural sodalite can be easily explained. As the pH of the distilled water rose toward 8.0, the rate of Na^+-H^+ exchange gradually decreased, until a constant value for the rate of the exchange reaction was attained. The pH value of 8.0 must therefore be the concentration at which the rate of Na^+ desorption is approximately the same as the rate of Na^+

adsorption in the reverse process.

This does not, however, explain why the minimum rate of dissolution should occur at a pH of 8.0. No satisfactory explanation exists at the present time to account for this minimum dissolution rate at a pH of 8. However, one possible explanation can be derived from the principle of the zero point of charge (Parks, 1967; Adamson, 1976). This principle has been used to explain many of the properties of colloidal suspensions in aqueous solutions, including their adsorption behavior. To understand what the zero point of charge is, it must first be remembered that the surface of a solid will have a net electrostatic charge due to the presence of many unbalanced chemical bonds. When immersed in an ionic solution, an electrostatic potential gradient will form in the immediate vicinity of the surface. Aqueous ions will be attracted to, or repelled from, this gradient depending on their charge. The net effect will be that a series of diffuse layers will form near the surface of the solid. This property has been quantified and is known as the electric double layer theory (Adamson, 1976). Although it is unnecessary to discuss the derivation of this theory in mathematical terms, it is important to be aware of its consequences.

The layer closest to the surface will consist of ions whose charge is opposite in sign to the sign of the surface charge. These ions may be in contact with discrete sites of excess charge on the surface. Above this layer is a more diffuse layer composed of ions with charges of opposite sign to the ions composing the first layer (Adamson, 1976). The end result will be a tendency for the surface charge to be neutralized by the formation of these ionic layers.

During the neutralization of the surface charge, large changes in the pH of the solution can occur (Parks, 1967). Thus the basis of the zero point of charge can be stated as follows: for a given surface composition and structure there is a pH value at which the surface charge is completely balanced. This presents us with part of the explanation for the shift in solution pH during the dissolution of natural sodalite. It is possible to quantitatively predict the zero points of charge for many oxides and silicates. Parks (1967) shows such calculations for many geologically relevant compositions. The accuracy of the calculations varies considerably, indicating that there are still factors which remain to be accounted for. In this study, it is not known what affect the presence of Cl^- anions in the lattice will have on the zero point of charge.

So far the pH dependence of silicate mineral dissolution has been demonstrated to have a sound theoretical basis. However, there is an explanation only for the adsorption of H^+ ions and the subsequent desorption of surface cations, Na^+ in the case of sodalite. The mechanism by which Al and Si are released to solution has not been identified. It should be recognized that the adsorption-desorption mechanism outlined above implies that the release of Al and Si occurs by a different mechanism than the release of Na. Such a mechanism has been suggested for feldspars by Aagaard and Helgeson (1982) and Helgeson et. al. (1985), and will be outlined below.

Aagaard and Helgeson (1982) believe that adsorbed H^+ ions as well as H^+ ions still in solution act to break apart the aluminosilicate framework, resulting in the release of fragments of the framework to solution. The activated surface sites are composed of part of the aluminosilicate structure which has been subjected to repeated H^+-Na^+ exchange of sufficient quantity to weaken the surrounding framework. Therefore the dissolving surface will have a variety of activated sites in different stages of decomposition.

Aagaard and Helgeson (1982) propose that the activated complex has the composition $(H_3O)AlSi_3O_8(H_3O)^+$ for solutions which are acidic. For more basic solutions, they propose that the activated complex has the composition $(H_3O)AlSi_3O_8(H_2O)$. In the case of an acidic solution it is the addition of the extra H_3O^+ radical which causes disruption of the framework, while the addition of H_2O causes disruption in basic solutions (Aagaard and Helgeson, 1982). This implies that the formation of the activated complex in acidic solutions will be quite dependent on the pH of the solution, while the solution pH has little effect in basic solutions. However, there is as yet little experimental evidence to support this hypothesis.

The difference in the nature of the empirical rate laws for Na and Si suggests that different mechanisms control the release of these two elements. This is supported by the theoretical discussion presented above. However, the results of the SIMS analyses have yet to be explained. The SIMS results suggest that a layer depleted in Na and Cl has formed at the surfaces of the samples, and that the thickness of this layer is dependent on time. This evidence suggests that diffusion of Na and Cl through the depleted layer may be responsible for the release kinetics of these two elements. Chemical diffusion has already been proposed as a mechanism for the dissolution of glasses in aqueous solutions (e.g. Isard et al., 1982). The following discussion will attempt to justify this explanation.

This discussion assumes that chemical diffusion of Na and Cl takes place in sodalite. Chemical diffusion is defined as the movement of a chemical species through a medium due to a difference in chemical potential of the species in the medium (Crank, 1975). The diffusion of Na and Cl through sodalite will form a concentration profile. Near the surface, the concentrations of these elements will be lowest, and will gradually increase with distance from the surface according to Fick's second law. Fick's second law may be expressed as:

$$dC_i/dt = -D(d^2C_i/dx^2)$$

This equation assumes that the change in the concentration of component i with time is related to the chemical potential gradient (expressed as the second derivative of concentration with distance) by a constant D, the diffusion coefficient. The minus sign indicates that the concentration change with time is decreasing if the concentration gradient is positive, i.e. the concentration increases with increasing distance.

To obtain an analytical solution of Fick's second law, the following boundary conditions must be assumed:

$C = C_o$ when x approaches infinity and at $t = 0$

$C = 0$ when $x = 0$ at $t > 0$

where C_o is the concentration of Na or Cl infinitely far from the interface ($x = 0$). Under these conditions, the solution to Fick's second law (Crank, 1975) is :

$$C_x/C_o = \mathrm{erfc}(x^2/4Dt)$$

for any given time t and distance x from the interface; the expression erfc(x) is the complement of the Gaussian error function of x. This solution is only valid if the diffusion coefficient D is constant over distance and time and the previously stated boundary conditions are satisfied.

Due to the nature of the SIMS analyses, a fully quantitative application of diffusion theory and methods could not be applied. Instead a more empirical method was devised to test whether or not diffusion could explain the SIMS profiles. The method will be explained below. The unprocessed SIMS profiles (e.g. counts/sec vs. sputter time) showed that the Si and Al profiles were essentially constant over the length of the profiles. This implies that the number of Si and Al atoms sputtered from the surface at any given depth is not dependent on the depth. Thus the number of Si and Al atoms at depth is simply the number of atoms present in unaltered sodalite. The Na and Cl profiles, however, show considerable variations in the number of atoms over the lengths of the profiles. If it is assumed that the Na and Cl profiles can be modelled by the diffusion equation, then the number of Na and Cl atoms can be calculated for any given depth.

If the number of Na and Cl atoms are calculated for a given depth and combined with the known constant number of Si and Al atoms, concentration profiles can be calculated independently of the actual SIMS profiles. This procedure is similar to the recalculation of SIMS profiles from raw data, although measurements are replaced by calculations (for Na and Cl) and known constant values (for Si and Al).

This procedure has been implemented in a computer program, and some of the results are shown in Figure 10b, along with an actual SIMS profile (Fig. 10a). There is remarkably good agreement for actual and calculated SIMS profiles for the synthetic brine experiments and for the 30 day distilled water experiment. However, discrepancies are apparent between the Si and Al actual and calculated results.

This analysis shows that diffusion of Na and Cl from

Figure 10. A comparison of an actual SIMS analysis of a natural sodalite wafer leached in distilled water for 30 days (a) and a modeled SIMS profile (b) for the same conditions as (a), assuming that the diffusion of Na and Cl from the surface produced the depletion of these elements, and that the relative enrichment of Si and Al in the surface is due to the depletion of Na and Cl only. Explanation of line styles:

solid line .... Na
dashed line .... Al
dash-dot line .... Si
dotted line Cl

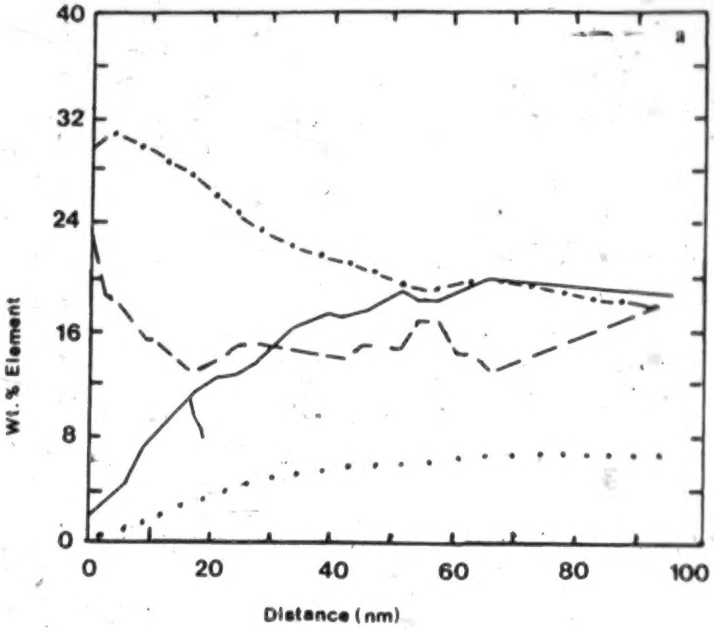
a
Wt.% Element
0
8
16
24
32
40
Distance (nm)
0
20
40
60
80
100

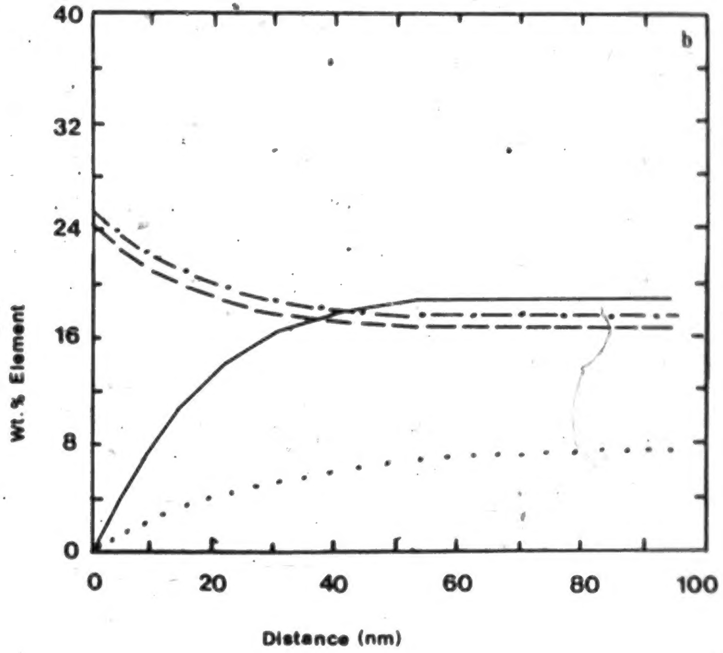
b
Wt.% Element
0
8
16
24
32
40
Distance (nm)
0
20
40
60
80
100

sodalite can explain some of the results of the SIMS analyses. However, it is apparent that the simple diffusion model used here does not adequately explain the results of the long duration experiments. There are also differences between the actual and calculated Si and Al profiles. The overall shapes of the calculated and actual Si and Al profiles are similiar although the calculated profiles are offset below the analyzed profiles. The discrepancies between actual and calculated results could be due in part to the simple diffusion model assumed here. The Na and Cl profiles from the 60 and 120 day experiments suggest that a diffusion model involving a moving interface or concentration dependent diffusion coeficients would be more applicable. However, no analytical or numerical solutions to the moving boundary problem were found for this study.

Two conflicting lines of reasoning have thus been developed in this study. The results of the dissolution experiments support the theory that dissolution occurs by some form of surface reaction. The SIMS results, on the other hand, indicate that diffusion of Na and Cl has occurred in a region close to the dissolving surface. The surface reaction theory has become the favored explanation in most recent studies of silicate mineral dissolution. In fact surface examination studies of leached silicate minerals (e.g. Holdren and Berner, 1978) have found only very thin altered layers, which indicate that diffusion is not the rate controlling process. This conclusion appears to be justified in the dissolution of sodalite. However, the results of this study also indicate that the dissolution process is quite complex and is likely composed of several distinct intermediate steps. As has been previously suggested, the release of Na, and probably Cl, occurs by a different mechanism than does the release of Si and Al. The release of Na has been assumed to be due to an exchange reaction with H^+ adsorbed onto the surface, while Al and Si are released by the decomposition of hydrated aluminosilicate complexes. The SIMS analyses suggest that the Na-H exchange reaction is not limited to the surface, but extends into the sample. However, diffusion from the sample is not the rate determining step in the release of Na, since this would produce a rate law for Na which has a square root dependence on time. Instead, the profiles could be explained if they represent the diffusion of H^+ into the sample. Since the release of Na will be controlled by the exchange reaction, a linear rate law will still be applicable if the diffusion of H^+ is rapid enough.

The apparent contradiction between the results of the dissolution experiments and the SIMS analyses can therefore be explained by a reaction mechanism which combines the surface reaction and diffusion hypotheses, with the rate determining step as part of the surface reaction.

Conclusion

The dissolution of natural sodalite in aqueous solutions has been found to be consistent with the results of other studies on the dissolution of silicate minerals. In particular, it has been found that the dissolution rate of sodalite in constant pH solutions is constant, and the experimental results can be fitted to a linear rate law. Experiments in distilled water, where pH was not buffered, resulted in rate laws with a logarithmic dependence on time for Na and Cl, and linear rate laws for Si and Al. The initial pH experiments indicated that at a pH of approximately 8.0, the dissolution rate of natural sodalite was minimal. Examination of the surfaces of leached samples shows that etching occurs rapidly in the first ten to fifteen days of dissolution, followed by an essentially constant state of surface reaction. The initial surface etching appears to occur on sites of weakness such as scratches and pits, but soon covers the entire surface with a fibrous appearance. In addition, the degree of etching of the sample surfaces is quite variable between samples and even on the surfaces of individual samples.

The results of the dissolution experiments were interpreted in terms of a complex surface mechanism involving three distinct stages:

1. The adsorption of H^+ ions onto specific surface sites.
2. An exchange reaction between adsorbed H^+ and Na^+,

resulting in the eventual release of Na^+.

3. The decomposition of the residual hydrated aluminosilicate lattice to release Si and Al.

The adsorption theory is consistent with a derivation presented by Lasaga (1981), which shows how the adsorption of H^+ can explain the observed fractional order of H^+ in dissolution rate laws. The observed minimum dissolution rate of sodalite at a pH of approximately 8.0 is explained in terms of the zero point of charge (ZPC). At a pH of 8.0, the surface charge of sodalite is balanced by the ionic composition of the aqueous solution. This results in a minimal rate of H^+ adsorption and hence a minimal rate of dissolution.

The release of Si and Al was explained by the decay of an unspecified hydrated aluminosilicate activated complex. Although the composition of the complex is unknown, there is evidence to suggest that it is similiar to that proposed for the dissolution of feldspars, namely $(H_3O)_4Al_3Si_3O_{12}(H_2O)$ (Aagaard and Helgeson, 1982; Helgeson et al., 1985).

The secondary ion mass spectrometry (SIMS) analyses suggested that diffusion of Na and Cl from the surfaces resulted in the formation of a leached layer near the surface. The Na and Cl profiles can be explained by applying Fick's second law of diffusion which assumes that the concentration of Na or Cl at a distance X from the surface and at time t is simply a function of the concentration gradient and the diffusion coefficient.

This hypothesis was tested by a simple model in which the results of the SIMS analyses were reproduced by assuming constant concentrations of Al and Si, and calculating the concentrations of Na and Cl by solving the diffusion equation for a given distance and time. The model reproduced the short duration experiments quite well, but significant discrepancies were found in the longer duration experiments. Although these results tend to support the theory that silicate minerals dissolve by a diffusion mechanism, there is no evidence for this in the results of the dissolution experiments. A diffusion mechanism would result in rate laws which have square root dependencies on time, which were not observed. Instead, the profiles were interpreted in terms of the penetration of H^+ into the sodalite, and the subsequent exchange of Na^+ and H^+. If the diffusion of H^+ into the sample and the diffusion of Na^+ out occur more quickly than the exchange reaction, then linear rate laws would still result. Therefore it is concluded that the dissolution of natural sodalite occurs by a complex mechanism which involves both surface reaction and diffusion, although the rate determining step is part of the surface reaction, and does not involve diffusion as some researchers propose.

There is an important implication for artificially produced sodalite for nuclear waste management. If sodalite has a minimum rate of dissolution at a pH of 8.0, then any steps taken to ensure that leaching solutions were at this pH would enhance the stability of sodalite in the storage site.

CHAPTER 4. THE DISSOLUTION OF IODOSODALITE

Introduction

The dissolution of iodosodalite has been previously considered by Winters (undated report) and Strachan and Babad (1979). Their results suggest that iodine is not preferentially leached from iodosodalite during dissolution. However, little work has been done on determining the actual kinetics of dissolution of iodosodalite. Strachan and Babad (1979) and Winters (undated report) performed dynamic "flow-through" experiments in which the leaching solution, distilled water, is continuously flushed over the sample. The results were cast into incremental leach rates with units of cm day^{-1}. As such, no kinetic results were obtained from these experiments. In addition, no consideration was given to the possible effect of residual NaI on the observed dissolution results.

The previous dissolution experiments on natural sodalite imply that the dissolution of iodosodalite should be strongly dependent on pH. If an analogy is drawn betweem the dissolution of natural sodalite and iodosodalite, it is expected that Na and I will be preferentially leached from the sample, leaving a Si-Al enriched layer. However, the presence of crystalline nepheline and very small amounts of residual NaI may affect the outcome of the experiments. In addition, it must be determined whether iodosodalite is stable in the synthetic brines. This chapter will describe a series of experiments designed to investigate these problems.

Sample Preparation

Iodosodalite for the dissolution studies was synthesized following the hot-pressing technique described in Chap. 2. A complete characterization of the product can be found in that chapter.

The final product consisted of a cylinder of iodosodalite approximately 3 cm in diameter and 10 cm in length. The cylinder was cut into several disks, each of approximately 2-5 mm in thickness. The surfaces of each disk were ground and polished down to 1 um grit. Geometric surface areas were calculated assuming a circular cross section. The diameters were measured on a micrometer stage equipped microscope with an accuracy of ±0.01 mm. The thickness of each disk was measured with a hand micrometer with an accuracy of ±0.01 mm. The cumulative error in the calculated surface area was ±0.05 cm^2.

Experimental Method

Before being used in an experiment, each disk was rinsed quickly in distilled water and ultrasonically rinsed in reagent grade acetone. The disks were stored in an oven at 110°C for at least 24 hours prior to experiments to evaporate any remaining surface moisture. Immediately before the beginning of an experiment, each wafer was weighed on a Mettler balance with an accuracy of ±0.00001g.

The wafers were completely immersed in the leaching solution so as to produce a sample surface area to solution volume ratio of 0.1 cm^{-1}. The samples were mounted on plastic frames with thin platinum wire for supports. It is estimated that greater than 95% of the surface area of each wafer was thus exposed to the leaching solution.

All experiments were conducted in tightly sealed Teflon containers. As soon as the sample was sealed in the container, it was immediately put into a one atmosphere oven set at a temperature of 50°C and left for the duration of the experiment. At the end of each experiment, the disk was removed from the solution, rinsed with distilled water and acetone and dried for at least 24 hours at a temperature of 110°C. The disk was then re-weighed and any weight changes were recorded.

The final solutions from the distilled water experiments were analyzed for Na, Al and Si using atomic absorption spectrometry and for I using a specific ion electrode. The final pH of the solution was measured with a pH electrode. Analyses of the synthetic brine compositions for Na, Al and Si was impossible because of their concentrated nature. An attempt was made to measure the dissolved I in the solutions from the brine experiments. Details of the analytical method can be found in Appendix 2.

Description of Experiments

All of the experiments conducted on iodosodalite were carried out under static "free drift" conditions; the leaching solution was not stirred or agitated and the pH of the solution was allowed to change without adjustment. Two different sets of dissolution experiments were conducted on samples of iodosodalite. These experiments are as follows:

1) Distilled water experiments: conducted at 50°C for durations of 1, 2, 5, 10 and 15 days. For the 1 d experiment, the water was heated to 50°C prior to beginning the experiment.

2) Synthetic brine experiments: conducted at 50°C for durations of 5, 10, 15 and 20 days. The synthetic brine composition used was SCSSS (Standard Canadian Shield Saline Solution). See Chapter 3 for the compositions of the synthetic brines.

The results of these experiments are shown in Table 10.

Results

The solution analyses were normalized to constant

Table 10. Iodosodalite dissolution experiments in distilled water.

Number	Duration (s)	R_{Na} x10^5	R_{Al} x10^8	R_{Si} x10^5	R_I x10^7
1	1286582	9.27	7.41	5.7	6.4
2	1286582	10	2.2	7.0	6.78
3	860371	5.31	1.48	4.0	5.44
4	860371	4.65	0.74	2.95	5.54
5	525225	5.18	0.74	3.74	5.37
6	525225	6.05	0.74	4.9	6.3
7	84000	4.44	2.97	2.4	1.66
8	178680	——	1.67	3.48	6.18

Units: R moles cm^{-2}

surface area, described as a reaction variable, R, with units of moles cm^{-2}. This normalization step eliminates the effect of varying surface areas and solution volumes between the different experiments, allowing direct comparison of the results.

Distilled water experiments

The normalized solution analyses are listed in Table 10and shown graphically in Fig. 11. The analyses show a rapid release of Na, Si and I in the first two days of experimentation followed by essentially constant release thereafter. The Al analyses show a high concentration afterone day but no further measurable amounts were found until after five days. The rate of Al release is constant after five days.

The release curves were fitted to a linear rate law by regression analysis. The calculated parameters for the linear rate laws are presented in Table 11. It is apparent from Fig. 11 and from Table 11 that the rate laws for Na and Si are quite similar, while the rate laws for Al and I are also similar. This observation is reflected in the values of the rate constants; the values for Na and Si are 5.53×10^{-11} moles $cm^{-2}s^{-1}$ and 2.37×10^{-11} moles cm^{-2} s^{-1} respectively. Similarly, the rate constants for Al and I are 2.2×10^{-14} moles cm^{-2} s^{-1} and 4.8×10^{-14} moles cm^{-2} s^{-1} respectively. These are

Figure 11. Normalized solution analyses for the dissolution of iodosodalite in distilled water:

a. Na

b. Al

c. Si

d. I

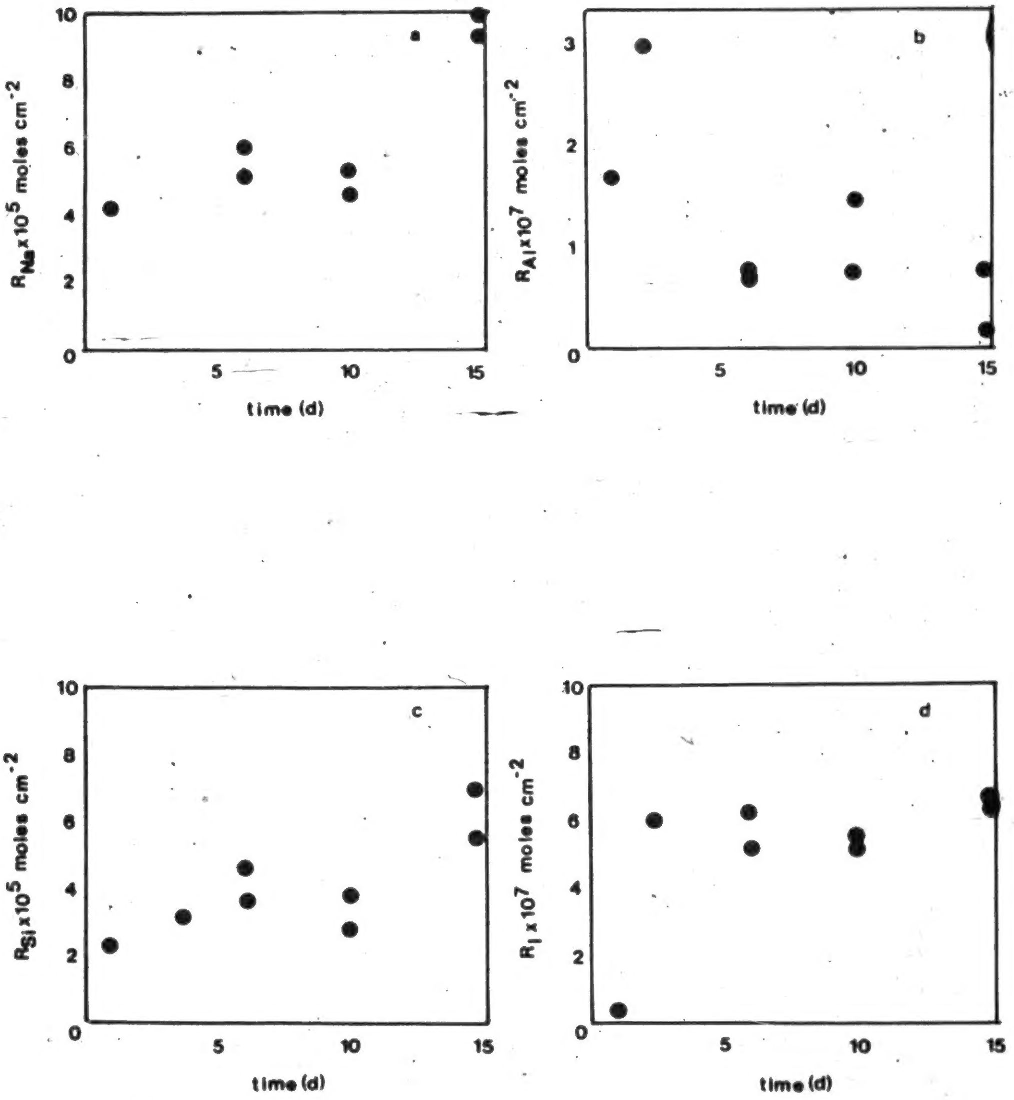
a
$R_{Na} \times 10^5$ moles cm^{-2}
0
2
4
6
8
10
5
10
15
time (d)
b
$R_{Al} \times 10^7$ moles cm^{-2}
0
1
2
3
5
10
15
time (d)
c
$R_{Si} \times 10^5$ moles cm^{-2}
0
2
4
6
8
10
5
10
15
time (d)
d
$R_{I} \times 10^7$ moles cm^{-2}
0
2
4
6
8
10
5
10
15
time (d)

Table 11. Rate law parameters for iodosodalite dissolution in distilled water

Na

$a = 1.82 \times 10^{-5}$

$b = 5.53 \times 10^{-11}$

$r = 0.82$

Al

$a = 1.02 \times 10^{-7}$

$b = 2.18 \times 10^{-14}$

$r = 0.15$

Si

$a = 2.67 \times 10^{-5}$

$b = 2.37 \times 10^{-11}$

$r = 0.68$

I

$a = 5.62 \times 10^{-7}$

$b = 4.83 \times 10^{-14}$

$r = 0.36$

units: a moles cm^{-2}; b moles cm^{-2} s^{-1}

quite different results than those obtained for natural sodalite, where the two different patterns of dissolution were for Na and Cl in one case and for Si and Al in the other case.

The weight change of the disks are all very similar within analytical error for all experiments. The percentage change in weight in all experiments was approximately 3.5-4.0%. This strongly implies that there is a period of initial dissolution followed by essentially constant slow dissolution.

The surface of a disk leached for 10 days was examined by SEM. A photomicrograph of the surface is shown in Plate 4a, along with the surface of a natural sodalite wafer (Plate 4b) leached in distilled water for the same time. This plate does not show any surface etching down to the resolution of the photograph. In contrast, the surface of the natural sodalite wafer leached for an identical time under identical conditions is deeply etched.

A SIMS analysis of a leached iodosodalite disk is shown in Fig. 12. The data for this figure were supplied in the recalculated atomic percent form; no further recalculation after the fashion of the natural sodalite analyses was performed. Figure 12 shows that the disk surface is depleted with respect to Na and Si to a depth of approximately 30 nm (15 min. sputter time). The Al and I

Plate 4. SEM microphotographs of an iodosodalite disk (a) leached for 10 days in distilled water, and a natural sodalite wafer surface (b) leached for 10 days in distilled water. The scale bar in each photograph is 10 um long.

A

B

Figure 12. SIMS analysis of an iodosodalite disk leached in SCSSS for 20 days. The analysis has been recast into atomic percent, and the horizontal scale is graduated in sputter time. The equivalent sputter distance is twice the sputter time.

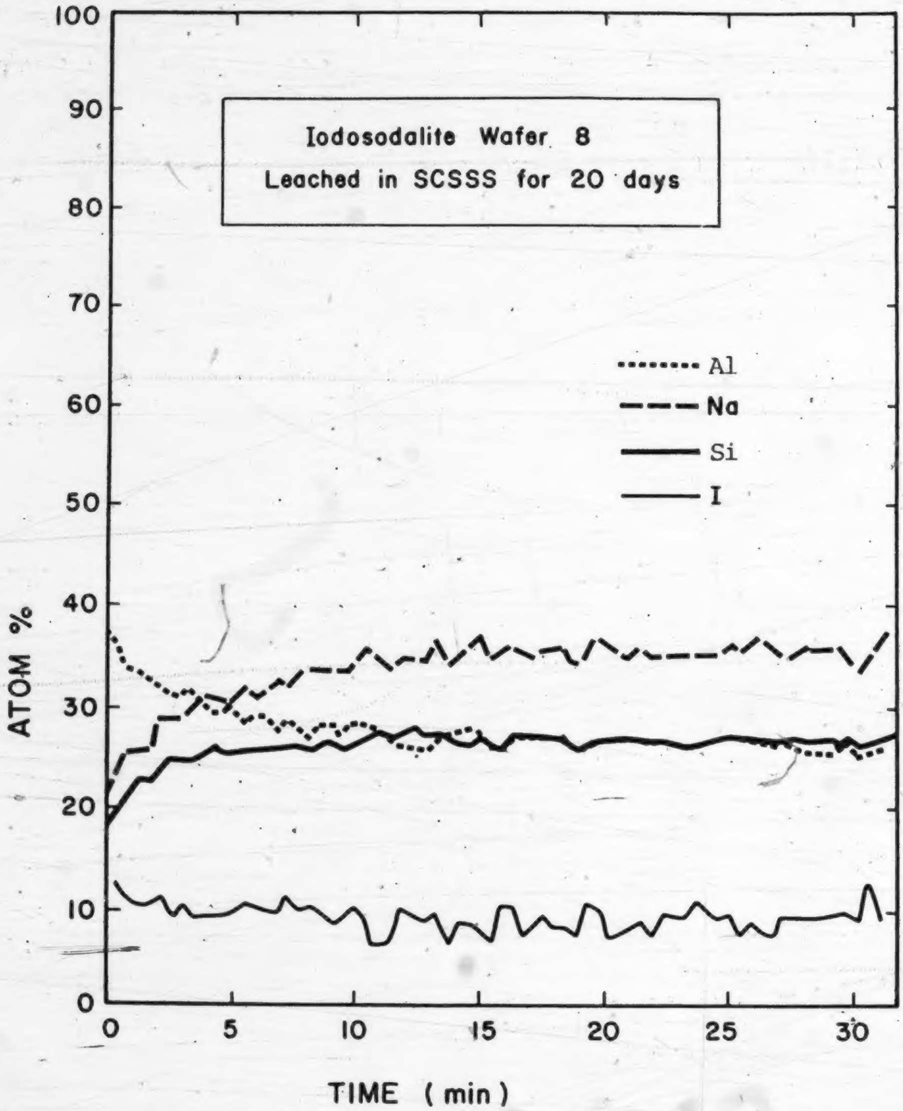
Iodosodalite Wafer 8
Leached in SCSSS for 20 days
Al
Na
Si
I
ATOM %
0
10
20
30
40
50
60
70
80
90
100
0
5
10
15
20
25
30
TIME (min)

profiles are constant over the depth of the analysis. This result is consistent with the results of the solution analyses, that Na and Si are preferentially leached from iodosodalite, while Al and I remain unleached.

Synthetic brine experiments

All of the brine experiments were conducted in the artificial brine composition known as Standard Canadian Shield Saline Solution (SCSSS). Since the brine has high concentrations of dissolved Na, Al and Si, it was not possible to analyze for the release of these elements from iodosodalite dissolution. However, several attempts were made to analyze for dissolved I^- by specific ion electrode. These analyses indicated that small quantities of I^- occurred in solution over and above the amounts normally found in SCSSS. The excess amounts were attributed to the release of iodine from iodosodalite.

Precise analyses of dissolved I^- in the SCSSS experiments proved to be impossible owing to the considerable variation in results between measurements on the same sample and between measurements on different samples. The variability in the measurements was attributed to interferences from dissolved Cl^- and S^{-2} in the SCSSS samples. Therefore no quantitative data were obtained for iodine release from iodosodalite in SCSSS. The weight changes for the iodosodalite disks were between 0.75 and

1.0% in all the brine experiments.

Discussion

The results of the distilled water experiments indicate that the dissolution behavior of iodosodalite is different than that of natural sodalite under similar conditions. These differences can be summarized as follows:

1. Similar rate laws for Na and Si and for Al and I; by analogy with natural sodalite Na and I would be similar, as would Si and Al.
2. Depletion of Na and Si in a surface layer. The results of the natural sodalite SIMS analyses imply that the surface layer should be depleted in Na and I.
3. No noticable surface alteration has occurred, such as was found on natural sodalite surfaces.

The similarity between the Na and Si rate laws and the occurrence of a surface layer depleted in Na and Si implies that a Na-silicate phase is being preferentially removed from iodosodalite. This is a reasonable possibility when it is remembered that small amounts of nepheline were observed in the hydrothermal synthesis experiments. Complete reaction of the NaI-nepheline mixture was not achieved during hot pressing and small amounts of the reactants would remain mixed in with the iodosodalite. Although no impurities such as Na-silicates were found, only small amounts would be required to produce the results obtained. The dissolution of a sodium silicate phase would also cause the pH of the solution to increase, as was observed in the distilled water experiments. In addition, the essentially constant weight changes observed in these experiments also imply that rapid dissolution of a very soluble phase has occurred. Thus the rapid release of Na and Si to solution and the existence of a surface layer depleted in Na and Si can be explained by the rapid dissolution of an Na-silicate.

Iodine also exhibits an initial rapid release to solution, although of a much smaller extent. This too can be explained if it is assumed that a small amount of I, probably in the form of NaI, remained in the iodosodalite and was preferentially leached out during the first stages of the experiments.

The preferential dissolution of a highly soluble phase does not completely explain the behavior of Al. The rapid decrease in the amount of Al in solution suggests both rapid release and precipitation as an insoluble phase. However, no further tests were undertaken to determine if Al was precipitating as an insoluble form.

After the initial rapid dissolution of the soluble phases, the slower dissolution of iodosodalite is represented by the rate laws of Al and I. The Na and Si rate laws are still dominated by the dissolution of the Na-silicate phase. If the rate constants for the linear portion of the Al and I release curves are taken as indicative of the rate of iodosodalite dissolution, then iodosodalite is much more durable than is natural sodalite under the same conditions. The rate constant for the release of I is an order of magnitude lower than the rate constant for Cl release under similar conditions (Fig. 4). In addition, I is not depleted in the surface of iodosodalite as is Cl in the surface of natural sodalite. In this sense iodosodalite is much more durable than natural sodalite under the same conditions.

The mechanism of dissolution of iodosodalite appears to be different than the mechanism for natural sodalite. The situation is greatly complicated by the simultaneous dissolution of the Na-silicate phase. Therefore it is difficult to compare these results with the natural sodalite dissolution results. However, several differences are apparent. The manner in which Cl and I are released to solution are different. Whereas the release of Cl is similar to that of Na and is probably associated with its release, the release of I is more closely related to that of Al. There is no readily apparent explanation for this difference in release between Cl and I.

Conclusions

These experiments confirm the results of Winters (undated) and Strachan and Babad (1979), that iodine is not being preferentially leached from iodosodalite. The dissolution of iodosodalite produced by hot pressing is dominated by two different processes. The dissolution of small amounts of an Na-silicate phase causes a rapid build-up of Na and Si in solution. This accounts for the rapid shift in solution pH toward 11. The preferential dissolution of Na and Si is noticable in the SIMS analysis of a disk leached in distilled water. This analysis also indicates that Al and I are not being preferentially leached from the surface. The SIMS analyses of disks leached in synthetic brines also do not show any preferential leaching of iodine. SEM photomicrographs of leached iodosodalite disk surfaces do not show any indication of the extensive etching present on natural sodalite surfaces.

It is apparent that iodosodalite is more durable than natural sodalite when subjected to similar leaching conditions. The steady-state release rate of iodine from iodosodalite is similar to that of chlorine from natural sodalite, although the total amount of I released is an order of magnitude less than the amount of Cl^- released. This is probably due to the lack of preferential leaching of I in the surface.

The results of the dissolution experiments indicate that iodosodalite is a promising candidate wasteform for the disposal of I-129. However, the results of these experiments must be included in a model which determines the long-term effects of the release of iodine from iodosodalite into the environment. Such a model must determine if the release rates of iodine from iodosodalite will result in unsafe concentrations of I-129 in the biosphere. This modelling is currently part of the Canadian nuclear waste management program. Therefore any assessment of the suitability of iodosodalite as a wasteform for I-129 must await the results of this modelling.

CHAPTER 5. CONCLUSIONS

It has been determined that iodosodalite can be synthesized under conditions of temperature and pressure that are readily accessible in an industrial setting. Iodosodalite containing between 10 and 15 wt. % I has been synthesized in a two stage process involving hot pressing of a nepheline gel-NaI mixture at 600-700°C and 400-500 bars pressure. The resulting iodosodalite has a density of 2.27 g cm^{-3}. The difference between this density and the theoretical density of 2.6 g cm^{-3} is attributed to residual pore space between grains. The hot-pressed iodosodalite contains minor amounts (< 1 wt. %) of nepheline and very small amounts of NaI.

The experimental synthesis of iodosodalite indicates that it can be synthesized over a variety of temperatures and pressures. The amount of iodine incorporated in iodosodalite is strongly dependent on the temperature of synthesis and on the time. Acceptable amounts of iodine incorporation were achieved after three days at 600°C and 500 bars.

The dissolution of natural sodalite was investigated to develop an understanding of the dissolution kinetics of sodalite. Dissolution was studied in distilled water, pH adjusted and buffered solutions, and in synthetic brine experiments. It was found that the dissolution of natural sodalite was strongly dependent on pH. A minimum degree of dissolution was found to occur at pH 8. Under buffered pH solutions, the rate of dissolution was found to obey linear rate laws. SEM examination of the surfaces of leached samples revealed rapid etching occurring in the first few days. Secondary ion mass spectrometric analyses of the surfaces indicated the existence of Na-Cl leached layers. The depth of the leached layer was found to be directly dependent on the length of the dissolution experiment; thicker layers resulted from longer experiments.

The dissolution of natural sodalite was explained by a two process model. The first process involves the adsorption of H^+ ions from solution onto the surface followed by exchange with surface Na^+ ions. This process left only the aluminosilicate framework on the surface. The H^+ ions also diffused into the sample and underwent exchange with Na^+ ions in the sample. This process resulted in the development of the leached layer, and could be partially modelled by diffusion of Na and Cl from within the sample.

The rate of H^+ adsorption is thought to be dependent on the electrostatic properties of the dissolving surface and the leaching solution. At a given pH, the rate of H^+ adsorption will be exactly balanced by the rate of H^+ desorption, thus resulting in the observed low rate of dissolution

The dissolution of iodosodalite was found to be quite different from the dissolution of natural sodalite. The release rates of Na and Si were very similar, as were those of Al and I. Analogy with natural sodalite indicated that Na and I should have shown similar rates of release. SIMS examination of the wafer surfaces showed that Na and Si were leached from the surface, while Al and I were not. SEM photomicrographs of disk surfaces leached in distilled water or synthetic brines did not show any evidence of extensive etching, as was found on natural sodalite surfaces. Iodosodalite is therefore more stable than is natural sodalite under similar leaching conditions.

The preferential release of Na and Si to solution was explained on the basis of the existence of small amounts of a soluble Na-silicate phase. This explains the similarity in the rates of Na and Si, but does not explain the lack of preferential leaching of I from iodosodalite. The low levels of iodine in solution combined with the SIMS results indicates that the iodine in iodosodalite is not readily released to leaching solutions.

This study has shown that iodosodalite can be readily synthesized from nepheline gel and NaI, and that large amounts of iodine can be incorporated using the hot pressing technique. The hot pressed iodosodalite has been shown to be much more resistant to leaching by aqueous solutions than natural sodalite. These results indicate that iodosodalite is a good candidate wasteform for the disposal of ^{129}I.

Bibliography

Aagaard, P. and H.C. Helgeson. 1982. Thermodynamic and kinetic constraints on reaction rates among minerals and aqueous solutions. I. Theoretical considerations. Amer. J. Sci. 282, p. 237-285.

Adamson, A.W. 1976. Physical chemistry of surfaces. John Wiley and Sons, New York. 698 p.

Appleman, D.E, D.S. Handwerker and H.T. Evans. 1963. The least-squares refinement of crystal unit cell with powder diffraction data by an automatic computer indexing method. Program, Ann. Mtg. Am. Cryst. Assoc., p. 42-43.

Barrer, R.M. and E.A.D. White. 1952. The hydrothermal chemistry of silicates. Part II. Synthetic crystalline sodium aluminosilicates. J. Chem. Soc. 1952, p. 1561-1571.

Barrer, R.M. and J.D. Falconer. 1956. Ion exchange in feldspathoids as a solid state reaction. Proc. Roy. Soc. (London) A236, p. 227-249.

Barrer, R.M., J.F. Cole and H. Stitcher. 1968. Chemistry of soil minerals. Part V. Low temperature hydrothermal transformations of kaolinite. J. Chem. Soc. (A) 1968, p. 2475-2485.

Barth, T.F.W. 1932. The structures of the minerals of the sodalite family. Zeit. Krist. 83, 405-414.

Berner, R.A. 1978. Rate control of mineral dissolution under earth surface conditions. Amer. J. Sci. 278, p. 1235-1252.

Berner, R.A. 1981. Kinetics of weathering and diagenesis. Mineral Soc. Amer. Reviews in Mineralogy vol. 8, Kinetics of Geochemical Processes (Eds A.C. Lasaga and R.J. Kirkpatrick), p 111-134.

Biggar, G.M. and M.J. O'Hara. 1969. A comparison of gel and glass starting materials for phase equilibrium studies. Min. Mag. 37, p. 198-205.

Bird, G.W. 1982. Selection and evaluation of buffer and backfill materials for use in a nuclear fuel waste disposal vault: the Canadian program. Proc. Workshop on Research and Development Needs Relating to Backfill for Underground Nuclear Waste Management. U.S. Natl. Bureau Stand., Gaitherburg, Md. (1981).

Brundle, C.R. 1982. Ultra-High vacuum techniques of surface characterization. In "Industrial Applications of Surface Analysis" (Eds. L.A. Caspar and C.J. Powell). Amer. Chem. Soc Symposium Series #199.

Boulton, J. 1978. Management of radioactive fuel wastes: the Canadian Disposal Program. Atomic Energy of Canada Report AECL-6314.

Boyd, F.R. and J.L. England. 1960. Apparatus for phase equilibrium measurements at pressures up to 50 kilobars and temperatures up to 1750°C. Jour. Geophys. Res. 65, p. 741-748.

Brundle, C.R. 1982. Ultra-high vacuum techniques of surface characterization. Amer. Chem. Soc.

Burger, L.L. 1980. Determining criteria for the disposal of iodine-129. Report, U.S. Dept. of Energy Contract DE-AC06-76RLO 1830. Pacific Northwest Laboratory, Richland, Washington.

Burger, L.L., R.D. Scheele and K.D. Wiemers. 1981. Selection of a form for fixation of Iodine-129. Report, U.S. Dept. of Energy Contract DE-AC06-76RLO 1830. Pacific Northwest Laboratory.

Busenberg, E. and C.V. Clemency. 1976. The dissolution kinetics of feldspars at 25°C and 1 atm CO_2 partial pressure. Geochim. Cosmochim. Acta 40, p. 41-49.

Chou, L. and R. Wollast. 1985. Study of the weathering of albite at room temperature and pressure with a fluidized bed reactor. Geochim. Cosmochim. Acta 48, p. 2205-2218.

Clark, W.E. 1977. The isolation of radioiodine with Portland cement. Part I: Scoping leach studies. Nucl. Tech. 36, p. 215-221.

Correns C.W. and W. von Engelhardt. 1938. Neue untersuchungen uber die Verwitterung des Kalifeldspates. Chem. d. Erde 12, p. 1.

Crank, J. 1975. The mathematics of diffusion, second edition. Clarendon press, Oxford, 414 p.

Deer, W.A., R.A. Howie and J. Zussman. 1963. Rock forming minerals, vol. 4. Framework silicates. Longman, London.

Dibble, W.E. and W.A. Tiller. 1981. Non-equilibrium water/rock interactions - I. Model for interface-controlled reactions. Geochim. Cosmochim. Acta 45, p. 79-92.

Edgar, A.D. 1973. Experimental Petrology: Basic principles and Techniques. Clarendon Press, Oxford.

Fleer, V.N. 1982. The dissolution kinetics of anorthite ($CaAl_2Si_2O_8$) and synthetic strontium feldspar ($SrAl_2Si_2O_8$) in aqueous solutions at temperatures below 100°C: with application to the geological disposal of radioactive nuclear wastes. Ph.D thesis, Pennsylvania State University.

Fritz, P. and S.K. Frape. 1981. Saline groundwaters in the Canadian Shield - a first overview. Chem. Geol. 36, p. 179-190.

Fung, P.C. and G.G. Sanipelli. 1982. Surface studies of feldspar dissolution using surface replication combined with electron microscope and spectroscopic techniques. Geochim. Cosmichim. Acta 46, p. 503-512.

Glasstone, S., K. Laidler and H. Eyring. 1941. The theory of rate processes. McGraw-Hill, New York. 600 p.

Grandstaff, D.E. 1977. Some kinetics of bronzite-orthopyroxene dissolution. Geochim. Cosmochim. Acta 41, 1097-1103.

Hamilton, D.L. and C.M.B. Henderson. 1967. The preparation of silicate compositions by a gelling method. Min. Mag. 36, p. 832-838.

Helgeson, H.C. 1971. Kinetics of mass transfer among silicates and aqueous solutions. Geochim. Cosmochim. Acta 35, p. 421-469.

Helgeson, H.C., W.M. Murphy and P. Aagaard. 1985. Thermodynamic and kinetic constraints on reaction rates among minerals and aqueous solutions. II. Rate constants, effective surface area, and the hydrolysis of feldspar. Geochim. Cosmochim. Acta 48, p. 2405-2432.

Holdren, G.R. and R.A. Berner. 1978. Mechanism of feldspar weathering - I. Experimental studies. Geochim. Cosmochim. Acta 43, p. 1161-1171.

Isard, J.O., A.R. Allnatt and P.J. Melling. 1982. An improved model of glass dissolution. Phys. Chem. Glasses 23, p. 185-189.

Lagache, M. 1976. New data on the kinetics of the dissolution of alkali feldspar at 200°C in CO_2 charged water. Geochim. Cosmochim. Acta 40, p. 157-161.

Lasaga, A.C. 1981. Chemical kinetics of water-rock interactions. Jour. Geophys. Res. 89 no. B6, p. 4009-4025.

Lasaga, A.C. 1981. Rate laws of chemical reactions. Mineral. Soc. Amer. Reviews in Mineralogy vol. 8. Kinetics of Geochemical Processes., p. 1-68.

Lemire, R.J. 1978. Disposal of Iodine-129. Atomic Energy of Canada Ltd. Memorandum RCB-78-067.

Luce R.W., R.W Bartlett and G.A. Parks. 1972. Dissolution kinetics of magnesium silicates. Geochim. Cosmochim. Acta 36, p. 35-50.

McKay, H.A.C., P. Miquel and I.F. White. 1981. Management modes for iodine-129. Report, European Atomic Energy Community, Management and Storage of Radioactive Wastes.

Paces, T. 1973. Steady-state kinetics and equilibrium between ground water and granitic rock. Geochim. Cosmochim. Acta 37, p. 2641-2663.

Parks, G.A. Aqueous surface chemistry of oxides and complex oxide minerals. Amer. Chem. Soc. Equilibrium Concepts in Natural Water Systems., p. 121-159.

Petrovich, R. 1976. Rate control in feldspar dissolution - II. The protective effect of precipitates. Geochim. Cosmochim. Acta 40, p. 1509-1521.

Prener, J.S. and R. Ward. 1950. J. Amer. Chem. Soc. 72, 2780-

Rimstidt, J.D. and H.L. Barnes. 1980. The kinetics of silica-water reactions. Geochim. Cosmochim. Acta 40, p. 1683-1699.

Schipper, D.J. and Th.W. Lathouwers. 1972. Bromine incorporation in sodalite. Inorg. Nucl. Chem. Letters 8, p 449-452.

Stormer, J.C., Jr. and I.S.E. Carmichael. 1971. The free energy of sodalite and the behavior of chloride, fluoride and sulfate in silicate magmas. Amer. Mineral. 56, p. 292-306.

Strachan, D.M. and H. Babad. 1979. Iodide and iodate sodalites for the long-term storage of iodine-129. Report RHO-SA-83, Rockwell Int. Corp., Richland, Wa.

Taylor, D. 1967. The sodalite group of minerals. Contrib. Mineral. Petrol. 16, p. 172-188.

Tomisaka, T. and H.P. Eugster. 1968. Synthesis of the sodalite group and subsolidus equilibria in the sodalite-noselite system. Min. J. 5, p. 249-275.

Van Peteghem, J. K. and B.J. Burley. 1963. Studies on solid solution between sodalite, nosean and hauyne. Can. Mineral. 7, p. 808-813.

Werner, H.W. 1975. The use of secondary ion mass spectrometry in surface analysis. Surface Science 47, p. 301-323.

Winters, W.I. undated. The effect of hot-pressing conditions on the properties of iodide sodalite. Rockwell Int. Corp. Informal Report RHO-LD-153.

Wollast, R. 1967. Kinetics of the alteration of K-feldspar in buffered solutions at low temperature. Geochim. Cosmochim. Acta 31, p. 635-648.

APPENDIX 1. THE GEL METHOD

The large scale synthesis of iodosodalite requires that large amounts of nepheline be produced. The normal method of producing nepheline involves mixing the oxides Na_2O, Al_2O_3 and SiO_2 in the correct stoichiometric proportions followed by several fusions at high temperature. Since nepheline melts at a high temperature (1560°C), special furnaces and platinum crucibles must be used. In addition, only small amounts of nepheline (< 5 g) can be synthesized at one time. To overcome these problems, an alternate method eas employed to produce large amounts of nepheline (> 15 g) at one time and without requiring high temperatures. A gel of nepheline composition can be synthesized from readily available materials.

The gel method of producing silicate compositions has been recognized for some time. Hamilton and Henderson (1967) and Biggar and O'Hara used the gel technique to produce silicate compositions suitable for phase equilibria studies. They reported that compositions of high purity could be rapidly produced with the gel method.

This method requires that an aqueous solution containing all of the required elements be produced. For nepheline gel, a solution containing Na and Al was produced by preparing 1.0M solutions of $NaNO_3$ and $Al(NO_3)_3.6H_2O$. Si was added to the nitrate solution in the form of tetraethylorthosilicate (TEOS, $C_5H_4SiO_4$). A sufficient quantity of ethyl alcohol was added to the nitrate-TEOS mixture to ensure complete miscibility.

The gel was produced by the addition of a small amount of NH_4OH to the mixture. This immediately caused the precipitation of aluminum hydroxide. The hydration of the TEOS occurred more slowly and was eventually responsible for formation of the gel. The mixture was sealed in a Nalgene bottle and left overnight to allow for complete hydration of the TEOS.

The gel was gradually dehydrated by heating in a water bath. Complete dehydration normally require two days. The result was a compacted powder of nepheline composition. The powder was fired in a Pt crucible over a bunsen burner to volatilize any remaining water and the nitrates present from the original solutions. The resulting powder was stored at 110°C to prevent adsorption of water vapor.

Some of the final powder was examined by X-ray diffraction, and was found to be completely amorphous. A small amount of the powder was fused to glass and analyzed for Na, Al and Si by electron microprobe. The analysis (Table A1) was found to be very close to the ideal nepheline composition. The slightly low Na composition is probably due to volatilization during the fusion. Thus the gel method was employed to produce large amounts of nepheline gel.

Table A1. Electron microprobe analysis of nepheline produced by the gel method

Oxide	Actual* wt. %	Theoretical wt. %
Na_2O	21.65	21.82
Al_2O_3	35.60	35.89
SiO_2	42.38	42.30

Analytical conditions: 15 kV operating voltage, 4 nA current, 60-240s counting time, under a rastered beam.

Analyst: D.B. Dingwell.

Appendix 2. Solution Analyses

Solutions from the dissolution experiments were analyzed for Na, Al and Si by atomic absorption spectrometry and for Cl^- or I^- by specific ion electrode. This appendix summarizes the procedures used to carry out the analyses.

The analyses for Na, Al and Si were performed on a Perkin-Elmer 503 Atomic Absorption Spectrometer set up for flame photometry. Na was analyzed by flame photometry using an air-acetylene flame. Al and Si were analyzed by flame photometry using an NO-acetylene flame.

A set of atomic absorption standards were prepared for Na and Si. The Na standards were prepared by serial dilution of a 1000 ppm Na stock solution. The Si standards were prepared by serial dilution of a 1000 ppm stock solution. Al standards were obtained from the standard collection of the atomic absorption laboratory.

Analyses were performed for Na, Al and Si by bracketing a sample analysis by a high and a low standard analysis. Multiple analyses were performed for each sample. Where necessary dilution of the samples was required. The sample composition was determined by linear interpolation between the bracketing standards. An estimate of analytical error was obtained by calculating the mean and standard deviation of the bracketed sample analyses. Typical analytical errors did not exceed 5-10%.

The Cl and I analyses were carried out by specific ion electrode. Standards for Cl and I were prepared according to the instructions in the accompanying instruction manual. Standards for Cl were prepared by serial dilution from a 1000 ppm Cl stock solution. Similarly, standards for I were prepared by serial dilution from a stock 1000 ppm I solution. A sufficient amount of 1.0M $NaNO_3$ was added to each standard to keep the ionic strengths constant.

Analyses of samples was carried out by bracketing each sample measurement with a high and low standard measurement. The electrode was allowed to stabilize in the solution before a measurement was taken. This required from one to five minutes, depending on the concentration of the standard and solution. The standard measurements were plotted on four-cycle semi-logarithmic graph paper. The logarithmic axis represented concentration while the linear axis represented measurements in mV. The standard measurements plotted on the graph so as to produce two parallel closely spaced curves. An approximation of analytical error was obtained by calculating the mean and standard deviation of the sample measurements against these two curves. Typical values for analytical error were approximately 10%.